U. S. DEPARTMENT OF THE INTERIOR

U.S. GEOLOGICAL SURVEY

# BASIN GEOLOGY OF THE UPPER SANTA CRUZ VALLEY, PIMA AND SANTA CRUZ COUNTIES, SOUTHEASTERN ARIZONA

by

M.E. Gettings and B.B. Houser[1]

Open-File Report 97-676



[1]U.S. Geological Survey, Southwest Field Office, 520 N. Park Ave., Rm. 355, Tucson, Arizona, 85719

## Contents



### Figures

**Plates** [plates are in pocket]



**Tables**



**Appendix**

## Abstract

The thickness, distribution, and character of alluvial sediments that were deposited in the subbasins of the upper Santa Cruz structural basin in southeastern Arizona during the late Tertiary provide important constraints on ground-water availability of the area. Two basin-fill units are recognized; the middle to late Miocene Nogales Formation and an unnamed Pliocene unit termed upper basin fill. Porosity and saturated bulk density for the two units were estimated using a combination of down hole gravimeter data from nearby bore holes in similar sediments, grain density measurements of cuttings, and surface gravimetric profiles. The calculated porosity of the Nogales Formation is 16 percent giving a saturated bulk density of 2.32 g/cc; the calculated porosity of the upper basin fill is 21 percent giving a saturated bulk density of 2.24 g/cc. These values agree qualitatively with the greater induration of the Nogales Formation observed in outcrop and the lower yields of water wells completed in the Nogales Formation compared to lesser induration and higher yields of the upper basin fill.

The complete Bouguer gravity anomaly map shows that four main subbasins make up the upper Santa Cruz structural basin. From north to south, these are the Amado, Tubac, Rio Rico, and Nogales subbasins. The Sopori subbasin (west of the Amado Subbasin) underlies Sopori Wash, a tributary of the Santa Cruz River. More exact locations and shapes of these subbasins, thickness of upper basin fill, and and depth to bedrock were estimated using a procedure involving interpolation of (1) the density functions derived in this study, (2) stratigraphic data from water wells, (3) a residual gravity anomaly grid obtained by subtracting the gravity effects of the bedrock ranges bordering the basin from the complete Bouguer gravity anomaly, and (4) depth to bedrock estimates from three NURE aeromagnetic profiles.

This procedure indicates that the subbasins are shallow and contain significant thicknesses of the Nogales Formation. For example, the Amado subbasin is estimated to contain about 300 m of upper basin fill and about 700 m of Nogales Formation. The Sopori subbasin contains about 50 m of upper basin fill and 650 m of Nogales Formation. The small thickness of upper basin fill in the subbasins is, in some cases, a function of tectonic uplift and erosion following deposition, but in other cases, the subbasins may have experienced only limited extension and subsidence after deposition of the Nogales Formation.

A number of previously unrecognized faults are indentified and known faults are extended using reconnaissance geologic mapping, study of driller's logs, interpretation of aerial photographs and thematic mapper satellite images, and inspection of contoured gravity and aeromagnetic anomaly data. Most faults that segment the main Santa Cruz basin and shape the boundaries of the subbasins are apparently pre-existing faults that have been reactivated by Basin and Range extension. One of these faults, the Mt. Benedict fault, controls the location of the Santa Cruz River as it crosses the

basin and affects the gradient of the floodplain. The effects of this fault and of other faults within the basin fill on ground-water movement should be investigated.

## Introduction

Population growth in the upper Santa Cruz Valley (both expansion within existing communities and the development of new communities) has the potential to exceed the available ground water of the area in the near future. State and local land-use planners need to know the location, thickness, depth, and estimated yield of the ground-water aquifers in the valley. Unfortunately there is little direct information about the thickness and depth of the aquifers in the valley because few deep wells to bedrock have been drilled.

The objective of this study is to use a combination of geologic and geophysical methods to determine the shapes and locations of the subbasins that make up the upper Santa Cruz basin, to describe the sediments that fill the subbasins, and to estimate the thickness of better consolidated lower basin-fill sediments (poor aquifers) relative to less consolidated upper basin-fill sediments (better aquifers) in the subbasins. The report is in two parts; the first part discusses the stratigraphy of the basin-fill sediments and the structures that control the subbasin shapes, and the second part describes the geophysical studies used to arrive at estimates of the shapes of the subbasins and thickness of basin fill.

## Location of study area

This report addresses the geology, structure, and ground-water potential of the subbasins that comprise the 50-km reach of the upper Santa Cruz Valley from the International boundary with Mexico to the confluence of the Santa Cruz River with Sopori Wash near Arivaca Junction (fig. 1). The ranges bordering the valley were studied only to correlate structures in the ranges with those inferred in the subbasins and to determine the provenance of clasts that make up the basin fill.

The Santa Cruz River has its headwaters in the San Rafael Valley in southeastern Arizona between the Huachuca Mountains and the Patagonia Mountains. The river flows southward into Sonora, Mexico about 30 km where it turns west around the southern end of the Sierra San Antonio and then flows back north toward Arizona, crossing the International boundary about 10 km east of Nogales. The course of the Santa Cruz is generally north between the International boundary and Tucson, a distance of about 110 km.

## Geologic Setting

The upper Santa Cruz River Valley is in the southern Basin and Range province of southeastern Arizona and northern Sonora. This terrain of alternating fault-bounded linear mountain ranges and sediment-filled basins began to form at about 17 Ma in southeastern Arizona as the result of

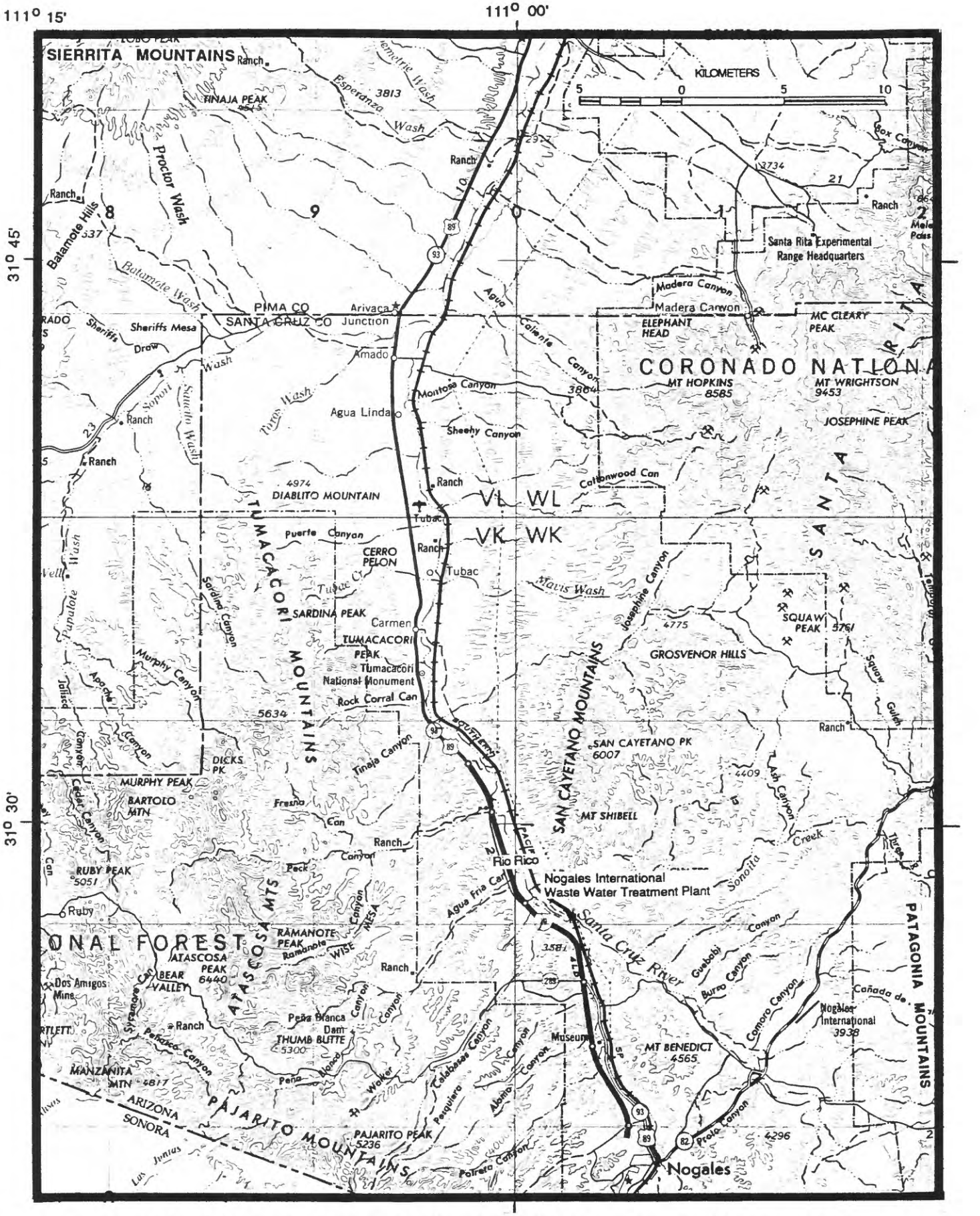


Figure 1. Map of the study area showing culture and physical features of the upper Santa Cruz Valley in Pima and Santa Cruz Counties, southeastern Arizona. Contour interval is 200 ft (61 m).

dominantly east-northeast/west-southwest directed crustal extension. The topography of the basins and ranges in this part of the province has a zigzag northeast and northwest pattern that may be a result of movement along west-northwest-trending Mesozoic faults that were reactivated by the Miocene extension.

The Santa Rita, San Cayetano, and Patagonia Mountains are on the eastern side of the upper Santa Cruz Valley (fig. 1). These mountains are made up of a variety of rocks including igneous, metamorphic, volcanic, and sedimentary rocks ranging in age from Precambrian to Miocene (Drewes, 1971, 1972, 1980) (fig. 2). Mount Wrightson in the Santa Ritas, at 2,881 m, is the highest point in the area.

The Tumacacori and Atascosa Mountains on the western side of the valley are composed chiefly of Tertiary volcanic rocks with the exception of a Jurassic granitic pluton south of Sopori Wash at the northern end of the Tumacacoris. The Pajarito Mountains at the southern end of the valley west of Nogales are composed of Cretaceous volcanics (Drewes, 1980). The mountains west of the valley are considerably lower than those to the east. Sardina Peak in the Tumacacoris is 1,712 m; Atascosa Peak in the Atascosa Mountains is 1,957 m.

The sedimentary rocks in the upper Santa Cruz Valley are Miocene to Holocene, chiefly alluvial sand and gravel deposits of fans, valley centers, terraces, and channels. On the basis of age and consolidation, these rocks can be separated into two basin-fill units overlain by surficial deposits as follows; (1) lower basin-fill unit or Nogales Formation, probably lower and middle Miocene, and poorly to moderately well consolidated, (2) upper basin-fill unit, upper Miocene to lower(?) Pleistocene, and unconsolidated to poorly consolidated, and (3) Pleistocene and Holocene surficial deposits including alluvium of stream channels, flood plains, and terraces, unconsolidated overall but locally well indurated.

## Acknowledgments

We gratefully thank the many people who assisted in collecting geologic and geophysical data for this project. Karen Baird and Paul Gettings established 83 new gravity stations in the study area. Cristina Bramley, Mark Bultman, Mary Hegmann, and Maurice Tatlow helped to establish the surface gravimetric profiles. Frederick Houser and Dorothy Houser assisted in the geologic mapping. Carol Finn assisted in obtaining a preliminary version of the 1996 aeromagnetic survey. The Arizona Geological Survey gave permission to measure densities of drill hole cuttings. The manuscript was greatly improved by the review of Floyd Gray. Funding for this project was provided in part by the Arizona Department of Water Resources.

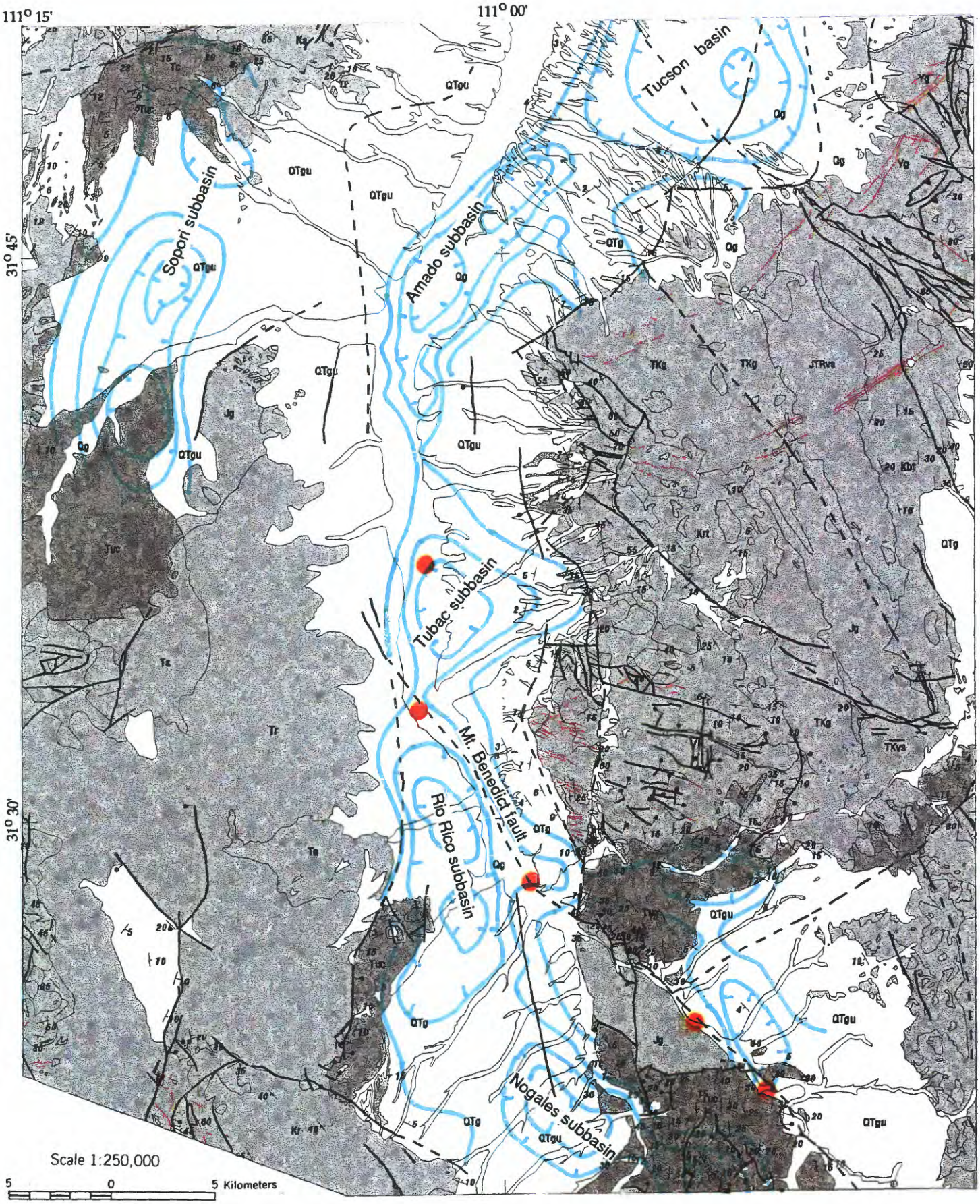


Figure 2. Generalized geologic map of the upper Santa Cruz Valley showing approximate location of subbasins based on complete Bouguer gravity anomaly map (plate 1). Gravity contour interval is schematic. Light shaded units are prebasin-fill rock; dark shaded unit is Nogales Formation; unshaded areas are upper basin fill and Quaternary alluvium. Orange dots indicate reaches of significantly higher gradient in the Santa Cruz River (table 1). Geology compiled by Drewes (1980) and modified by Houser (unpublished data).

# Part 1. Geological Investigations

## Data sources

The information and interpretations in the geologic part of this report are based on previous geologic mapping by U.S. Geological Survey geologists and University of Arizona graduate students, and on reconnaissance mapping of the present study. Drillers' logs of 97 water wells were examined and interpreted as to the units that were penetrated. Cuttings of about 40 wells, stored at the Arizona Geological Survey in Tucson, were examined. For a few wells, logs and cuttings are both available. Color infrared aerial photographs at a scale of 1:60,000, black and white photos at 1:40,000, and thematic mapper satellite images were used in reconnaissance geologic mapping and interpretation of the structure of the piedmont areas of the valley.

Future work as part of the continuing geologic investigation of the upper Santa Cruz Valley will include detailed geologic mapping in areas critical to the interpretation of basin-fill stratigraphy and subbasin margins. Samples of some of the tuffs interbedded at the base of the Nogales Formation have been submitted for $^{40}Ar/^{39}Ar$ dating. Thematic mapper satellite images of the upper Santa Cruz Valley will be studied further for structural information and additional well logs will be acquired.

## Stratigraphy of the Basin Fill

Basin-fill sediments of the southern Basin and Range province are usually defined as the detritus that accumulated in structural basins that had more or less the modern configuration. This definition eliminates mid-Tertiary conglomerate units, such as the Pantano Formation (Balcer, 1984), that were deposited in basins different than the modern ones, and volcaniclastic conglomerates interbedded with lava and ash flows in the ranges.

At least two ages of basin fill can be distinguished in most basins in southeastern Arizona (Houser and others, 1985; Dickinson, 1991). The older basin-fill beds may be mildly to moderately deformed with dips of 10° to 45°; locally, adjacent to range front faults for example, bedding can be nearly vertical. Younger basin-fill beds commonly display only initial dips of less than 5°. The older basin fill is usually better consolidated and is denser than the younger basin fill. The consolidation and greater density result from diagenetic processes that alter the mineralogy of the matrix of the sediment and fill pore spaces. It is chiefly the reduction in pore space and resultant decrease in permeability that makes the older basin-fill sediments poor aquifers compared to the younger basin-fill sediments. Another difference between the two ages of basin fill that is useful in mapping the units is that older fill commonly contains clasts of lithologies that are no longer present in the immediately adjacent ranges. In most cases this is simply a consequence of erosional stripping where the uppermost rocks of the ranges are removed

first and are, thus, deposited as the oldest basin sediments. In some cases significant offset along faults may be involved in bringing diverse bedrock lithologies in juxtaposition with basin sediments.

**Nogales Formation (lower basin fill)**

Most of the outcrop areas of the lower basin-fill units in the upper Santa Cruz Valley, including the valleys of Nogales Wash and Sopori Wash, were identified in geologic mapping by Nelson (1963), Drewes (1971, 1972, 1980), Cooper (1973), and Simons (1974). The names given to these lower units were the Pena Blanca Formation (Nelson, 1963), the middle member of the Tinaja Peak Formation (Cooper, 1973), and the Nogales Formation (Drewes, 1971, 1972; Simons, 1974). In this report the name Nogales Formation is used for all the lower basin-fill units in the upper Santa Cruz drainage basin. This usage is restricted to lower basin-fill units younger than about 17 Ma and, therefore, excludes older volcaniclastic conglomerate units interbedded with mid-tertiary volcanic rocks found within the ranges.

Distribution. The lower basin-fill units are widely exposed at a number of sites around the Santa Cruz Valley near the lower slopes of the mountains (figs. 1, 2); for example south of the Sierrita Mountains, in the valley of Sopori Wash, between Sonoita Creek and Mt. Benedict, and between Nogales and the Santa Cruz River south of Mount Benedict. Smaller exposures are east of the Atascosa Mountains in Walker, Pena Blanca and Agua Fria Canyons, and west of the Santa Rita Mountains in Cottonwood Canyon and other canyons. Excellent descriptions of the Nogales Formation were given by Drewes (1972) for exposures west of the Santa Rita and San Cayentano Mountains and by Simons (1973) for the exposures north and south of Mt. Benedict. Although the lower basin fill differs in detail at different exposures around the basin, it was correlated across the basin by Drewes (1973, 1980) and Simons (1974) based on general similarity of appearence and consolidation.

Age and contacts. In the upper Santa Cruz Valley, the Nogales Formation is in fault contact with pre-Cenozoic rocks and is in fault or depositional contact with Oligocene and lower Miocene volcanic rocks. It commonly rests on or is interbedded with ash-flow or airfall tuff beds near its base. It was probably the presence of airfall tuff interbeds at the base of the Nogales Formation south of the Sierritas that led Cooper (1973) to include part of the Nogales conglomerate in the middle member of his predominantly volcanic Tinaja Peak Formation (K-Ar ages of 24 Ma to 26.4 Ma). Drewes (1980) reinterpreted the conglomerate as overlying the Tinaja Peak Formation and this interpretation is borne out in excellent new exposures in the Caterpillar testing grounds northwest of Tinaja Peak. Stratigraphically, usage of the middle member of the Tinaja Peak Formation is restricted to conglomerate beds interbedded with silicic flows on the east side of Tinaja Peak.

The thickness of the tuffs at the base of the Nogales Formation varies considerably. For example, an airfall tuff presumed to be near the base of the

Nogales in Cottonwood Canyon west of the Santa Rita Mountains is less than 2 m thick, whereas an ash-flow tuff interbedded with conglomerate in Walker Canyon east of the Atascosa Mountains is about 25 m thick. No radiometric ages have been obtained for tuffs associated with the Nogales in the upper Santa Cruz Valley nor have there been any attempts to correlate the various tuff beds based on phenocryst content. A basalt flow interbedded in the lower half the Nogales Formation northwest of Agua Fria Canyon yielded a K-Ar age of 12.6±0.8 Ma on the groundmass (Drewes, 1972; Simons, 1974).

In the few places where it is exposed, the contact of the Nogales Formation with the overlying upper basin-fill sediments is gradational within an interval of about 50 m. The transition is marked chiefly by a decrease in consolidation upward and an increase in the lithologic variety of the clasts.

General appearance and thickness. The Nogales Formation is a pale red to grayish pink conglomerate, commonly tilted at 5° to 15°, that typically supports steep hillslopes and vertical banks or cliffs along washes. Clasts are angular to subangular; sorting is poor to moderate; grain size ranges from silt to boulders as much as 2 m across, with sandy grit, pebbles, and cobbles being the most common sizes. Bedding is moderate to good in pebbly and sandy intervals and current cross bedding is locally present. In cobbly to bouldery intervals, bedding is generally poor.

The formation is only moderately well consolidated except near the base where it is locally very well consolidated. Cementing is variable and is mostly noncalcareous to slightly calcareous. Considering that for the most part the Nogales is only moderately well consolidated, it forms some surprisingly high cliffs. For example, on the south side of Cottonwood Canyon west of the Santa Ritas it forms a vertical cliff 36 m high, yet pebbles and cobbles can be pulled from the face of the cliff by hand. The matrix of the conglomerate appears to be tuffaceous, especially near the base of the unit where tuff beds are common. Exposures that look the most tuffaceous also tend to have poorly developed thick bedding and matrix supported clasts, some boulder size.

Simons (1974) estimated the thickness of the Nogales Formation to be about 2,285 m between Nogales and the Santa Cruz River where he separated it into lower, middle, and upper members. Nelson (1963) gave the thickness of his Pena Blanca Formation as about 110 m, but he showed it to be more than 250 m thick on his cross section. South of the Sierrita Mountains, the calculated combined minimum thickness of the Nogales Formation and Cooper's (1973) middle member of the Tinaja Peak Formation is 630 m. In Cottonwood Canyon west of the Santa Ritas, the calculated minimum thickness of the Nogales is about 850 m. All these thicknesses may be correct for their particular location and may represent different depositional settings.

Clast composition. In most places the Nogales Formation is a conglomerate composed of predominantly volcanic clasts. Other clasts, such as granitic

rocks, and Paleozoic sandstone and limestone, commonly make up less than 5 to 10 percent of the conglomerate, although granitic detritus is locally abundant. Simons (1974) reported that, along the Santa Cruz River south of Route 82, the Nogales Formation is a coarse granitic fanglomerate that grades westward toward the town of Nogales into epiclastic volcanic conglomerate containing minor granitic clasts. Reconnaissance study of exposures north and west of the Batamote Hills (about 5 to 7 km southwest of exposures of the Nogales Formation south of the Sierritas) (figs. 1, 2) shows that well consolidated conglomerate there contains abundant granitic clasts.

As noted by Drewes, on the western side of the Santa Ritas the overwhelming preponderance of clasts in the Nogales Formation are derived from the Oligocene Grosvenor Hills Volcanics (Drewes, 1972). This implies that when the conglomerate was being deposited the Santa Ritas were still mantled by Cenozoic volcanic rocks. Nelson (1963) noted that on the western side of the Santa Cruz Valley (east of the Atascosa Mountains) most clasts in his Pena Blanca Formation were representative of the volcanic rocks of the area, but some clasts were of lithologies not exposed anywhere nearby.

Depositional environment. Based on grain size, sorting, and bedding, most of the Nogales Formation was probably deposited in alluvial fans similar to those of the modern upper Santa Cruz Valley. Clast imbrication indicates that the detritus was shed off ranges on the east and west and carried toward the center of the valley. Based on limited well data, there do not seem to be any playa or lacustrian facies at depth along the axis of the valley. The absence of playa or lacustrine facies suggests that the basin was not closed during deposition of the Nogales Formation. It was likely drained by a north- or south-flowing axial stream.

**Upper basin fill**

The upper basin-fill sediments of the upper Santa Cruz Valley are chiefly coarse- to medium-grained, gravelly alluvial fan deposits derived from the adjacent ranges. Like the underlying Nogales Formation, no lacustrian or playa facies have been identified in the upper basin fill, either in outcrop or in drillers' logs of water wells, which implies that the upper Santa Cruz Valley was never a closed basin. The basin-center facies of the upper basin fill may be represented by fine-grained pebbly mudstone exposed locally in the bluffs on the east side of the Santa Cruz River.

Descriptions of the upper basin-fill sediments on the west side of the Santa Rita Mountains were given by Drewes (1972) and Helmick (1986). The upper basin fill in the rest of the Santa Cruz Valley is similar. It is unconsolidated to poorly consolidated, although it is locally well cemented with calcite; clasts are subangular to subrounded; sorting and bedding are poor to good. The composition of the clasts reflects the lithologies currently exposed in the adjacent ranges as opposed to the clasts in the Nogales Formation which, in part, reflect the stripping of the mid-Tertiary volcanic cover from the Santa Rita Mountains.

The thickness of the upper basin fill ranges from a few meters where it laps up onto the bedrock on the sides of the Santa Cruz Valley to about 260 m (well log shown by Drewes, 1980) in the Amado subbasin. The upper basin fill is thicker to the north. Drillers' logs indicate that 13 km north of Arivaca Junction the upper basin fill is more than 365 m thick.

There are no datable materials in the upper basin fill and no fossils have been found. Tuff beds near Alum Canyon that Drewes (1971, 1972) included in the base of the upper basin fill are interpreted in this study to be at the base of the Nogales Formation. Based on similarities of appearance and consolidation with sediments in other basins in the southern Basin and Range that contain datable materials, the age of the upper basin fill is estimated to be upper Miocene, Pliocene, and lower(?) Pleistocene. The upper basin fill in the Santa Cruz basin has not been given a formal stratigraphic name.

## Structure

The upper Santa Cruz Valley is one of the narrower valleys in southern Arizona (only 8 to 12 km wide) suggesting that the basin it overlies has undergone only minor to moderate lateral extension during the late Cenozoic. Because there is a general positive correlation between basin width, amount of extension, and basin depth, the narrowness of the valley probably also means that the basin is shallow. Other indications that the upper Santa Cruz basin is shallow are (1) the Bouguer gravity anomalies over the basin are not very low (see Part 2 of this report), (2) there are no lacustrian or playa sediments in the basin fill indicating that the basin was never closed, and (3) extensive outcrops of the Nogales Formation south of the Sierritas, in the valley of Sopori Wash, and north and south of Mt. Benedict suggest that basin subsidence in some of these areas stopped after the Nogales Formation was deposited (Sierritas and Sopori Wash), while other areas have undergone uplift and the upper basin fill has been removed by erosion (Mt. Benedict).

### Subbasins

The complete Bouguer gravity anomaly map of the upper Santa Cruz Valley (pl. 1) shows that, beneath the basin fill, the Santa Cruz basin is comprised of a string of four northeast-, north-, and northwest-trending relatively small subbasins separated from each other by saddles (fig. 2). For the purposes of this report, from north to south the subbasins are named the Amado, Tubac, Rio Rico, and Nogales subbasins. Between the communities of Arivaca Junction and Rio Rico, the course of the Santa Cruz River more or less coincides with the trend of the buried subbasins. South of Rio Rico, however, the Santa Cruz River goes to the east of Mt. Benedict whereas the deeper subbasins underlie the valley of Nogales Wash on the west side of Mt. Benedict. The subbasins and the course of the river probably join again just south of the International boundary, but gravity data for Sonora are not available to substantiate this. The map also shows a north-northeast-trending subbasin between Sopori Wash and the Sierrita Mountains (the Sopori

subbasin), and two small unnamed subbasins south of Sonoita Creek and east of Mt. Benedict.

**Structural control of the upper Santa Cruz River**

Structural control of the course of the upper Santa Cruz River can be readily seen in the stretch of the river between the border and the Nogales International Waste Water Treatment Plant (fig. 2). Here the river channel is in bedrock and follows a north-45°-west-trending fault (herein called the Mt. Benedict fault) that separates the Mt. Benedict quartz monzonite and Nogales Formation on the southwest from Nogales Formation and upper basin-fill sediments on the northeast (Simons, 1974). The Bouguer gravity (pl. 1) and aeromagnetic anomaly (fig. 9) maps indicate that the fault continues beneath the basin fill along strike to the northwest and crosses the upper Santa Cruz basin at an oblique angle. This is the course that the Santa Cruz River takes across the basin, which strongly suggests that the Mt. Benedict fault also controls the location of this part of the river. The fault separates the Rio Rico and Tubac subbasins and emerges on the western side of the valley at the base of Tumacacori Peak where it continues on to the northwest into the Tumacacori Mountains.

The sense of movement on the Mt. Benedict fault is variable from place to place. Where the fault is exposed south of the Nogales International Waste Water Treatment Plant, the movement is down on the northeast. Where the fault passes beneath the upper Santa Cruz basin, the sense of movement is inferred to be down on the west on the northeast side of the Rio Rico subbasin; between the Rio Rico and Tubac subbasins the fault may act as a transfer fault. Drillers' logs show that where the fault continues northwest into the piedmont slope of the Tumacacori Mountains, it forms the eastern side of a small graben next to the mountain and that it has about 100 m of displacement here, down on the west.

**Upper Santa Cruz River gradient and Quaternary faulting.**

The longitudinal gradient (ratio of elevation change to distance) of the upper Santa Cruz River was calculated from near Canoa Ranch (about 8 km north of Arivaca Junction) to a point about 5.5 km south of the international border (table 1). The measurements were made between elevations of 887 m (2910 ft) and 1160 m (3806 ft) using U.S. Geological Survey 7 1/2 ' topographic maps. The straight line distance between each point where a contour line crossed the river was used to calculate the gradient, rather than the actual channel distance between contour intervals. Because rivers commonly develop meandering channels as an adjustment to gradient increases, eliminating the meanders by measuring straight line distances emphasizes gradient increases and gives a better picture of the slope of the flood plain.

Table 1. Gradients of the upper Santa Cruz River between 887 m (2,910 ft) and 1,160 m (3,806 ft). [Gradient = elevation change divided by distance.]

| Quadrangle | Elevation interval (ft) | Distance (ft) | Cumulative distance (mi) | Cumulative distance (km) | Gradient |
|---|---|---|---|---|---|
| Esperanza Mill | 2,910-2,920 | 2,798 | 0.53 | 0.85 | .0036 |
| --------do-------- | 2,920-2,930 | 3,379 | 1.17 | 1.88 | .0030 |
| --------do-------- | 2,930-2,940 | 2,482 | 1.64 | 2.64 | .0040 |
| --------do-------- | 2,940-2,950 | 2,640 | 2.14 | 3.44 | .0038 |
| --------do-------- | 2,950-2,960 | 2,904 | 2.69 | 4.33 | .0034 |
| --------do-------- | 2,960-2,970 | 2,218 | 3.11 | 5.00 | .0045 |
| --------do-------- | 2,970-2,980 | 3,802 | 3.83 | 6.16 | .0026 |
| Amado | 2,980-3,000 | 3,538 | 4.50 | 7.24 | .0028 |
| --------do-------- | 3,000-3,010 | 2,851 | 5.04 | 8.11 | .0035 |
| --------do-------- | 3,010-3,020 | 3,062 | 5.62 | 9.04 | .0033 |
| --------do-------- | 3,020-3,030 | 2,746 | 6.14 | 9.88 | .0036 |
| --------do-------- | 3,030-3,050 | 4,646 | 7.02 | 11.30 | .0043 |
| --------do-------- | 3,050-3,070 | 5,702 | 8.10 | 13.03 | .0035 |
| --------do-------- | 3,070-3,080 | 3,221 | 8.71 | 14.01 | .0031 |
| --------do-------- | 3,080-3,090 | 1,954 | 9.08 | 14.61 | .0051 |
| --------do-------- | 3,090-3,100 | 2,323 | 9.52 | 15.32 | .0043 |
| --------do-------- | 3,100-3,120 | 6,336 | 10.72 | 17.25 | .0032 |
| --------do-------- | 3,120-3,130 | 3,221 | 11.33 | 18.23 | .0031 |
| --------do-------- | 3,130-3,140 | 3,062 | 11.91 | 19.16 | .0033 |
| --------do-------- | 3,140-3,150 | 2,376 | 12.36 | 19.89 | .0042 |
| --------do-------- | 3,150-3,160 | 5,122 | 13.33 | 21.45 | .0020 |
| Tubac | 3,160-3,180 | 3,379 | 13.97 | 22.48 | .0059 |
| --------do-------- | 3,180-3,200 | 2,851 | 14.51 | 23.35 | .0070 |
| --------do-------- | 3,200-3,220 | 7,761 | 15.98 | 25.71 | .0026 |
| --------do-------- | 3,220-3,240 | 4,118 | 16.76 | 26.97 | .0049 |
| --------do-------- | 3,240-3,260 | 6,019 | 17.90 | 28.80 | .0033 |
| --------do-------- | 3,260-3,280 | 3,221 | 18.51 | 29.78 | .0062 |
| --------do-------- | 3,280-3,300 | 4,963 | 19.45 | 31.30 | .0040 |
| --------do-------- | 3,300-3,320 | 5,702 | 20.53 | 33.03 | .0036 |
| --------do-------- | 3,320-3,340 | 4,858 | 21.45 | 34.51 | .0041 |
| --------do-------- | 3,340-3,360 | 4,277 | 22.26 | 35.82 | .0047 |
| Rio Rico | 3,360-3,380 | 6,600 | 23.51 | 37.83 | .0030 |
| --------do-------- | 3,380-3,400 | 5,386 | 24.51 | 39.44 | .0037 |
| --------do-------- | 3,400-3,420 | 2,578 | 25.02 | 40.26 | .0077 |

| | | | | | |
|---|---|---|---|---|---|
| --------do------- | 3,420-3,440 | 5,597 | 26.08 | 41.96 | .0036 |
| --------do------- | 3,440-3,460 | 5,808 | 27.18 | 43.73 | .0034 |
| --------do------- | 3,460-3,480 | 6,706 | 28.45 | 45.78 | .0030 |
| --------do------- | 3,480-3,500 | 5,280 | 29.45 | 47.39 | .0038 |
| --------do------- | 3,500-3,520 | 4,910 | 30.38 | 48.88 | .0035 |
| --------do------- | 3,520-3,540 | 4,435 | 31.22 | 50.23 | .0045 |
| --------do------- | 3,540-3,560 | 2,904 | 31.77 | 51.12 | .0069 |
| --------do------- | 3,560-3,580 | 5,016 | 32.72 | 52.65 | .0040 |
| Cumero Canyon | 3,580-3,600 | 4,013 | 33.48 | 53.87 | .0050 |
| --------do------- | 3,600-3,620 | 4,224 | 34.28 | 55.16 | .0047 |
| --------do------- | 3,620-3,640 | 4,013 | 35.04 | 56.38 | .0050 |
| Kino Springs | 3,640-3,680 | 3,590 | 35.72 | 57.47 | .0111 |
| --------do------- | 3,680-3,700 | 7,180 | 37.08 | 59.66 | .0028 |
| --------do------- | 3,700-3,720 | 7,392 | 38.48 | 61.91 | .0027 |
| --------do------- | 3,720-3,740 | 4,277 | 39.29 | 63.22 | .0047 |
| --------do------- | 3,740-3,806 | 15,206 | 42.17 | 67.85 | .0043 |

The average gradient of the upper Santa Cruz is .0041 $\pm$.0016 along this 68 km stretch of the river. The gradient is quite uniform and exceeds the average gradient by more than one standard deviation at only five places. There is only one reach where the gradient is lower than the average by one standard deviation, probably because the river readily fills in low gradient areas with sediment during floods. The one reach that has a low gradient is directly downstream from a high-gradient reach near Tubac and, thus, may reflect adjustment by the river to the high-gradient reach.

Figure 2 shows that the three high-gradient reaches in the alluvial part of the river channel are located where the river encounters the edge of a subbasin or a node between two subbasins. The gradient at the northern edge of the Tubac subbasin is .0064; on the node between the Tubac and Rio Rico subbasins it is .0062; and at the eastern edge of the Rio Rico subbasin it is .0077. The other two river reaches with high gradients are located in the bedrock part of the channel on the Mt. Benedict fault and, thus, may be caused by heterogeneities in the bedrock. The gradient of the reach just south of Burro Canyon is .0069; the gradient associated with the meanders near Kino Springs is .0111.

The association of subbasin boundaries with gradient increases in the alluvial part of the river channel may indicate that differential tectonic movement associated with the boundaries of the subbasins is still taking place and, moreover, that this differential movement is being transmitted to the surface along faults in the basin-fill sediments. This has significance for the analysis of ground-water flow in the aquifers of the upper Santa Cruz basin

because some faults may restrict the movement of groundwater, whereas others may channel or enhance ground-water movement.

Additional evidence that the subbasins are still subsiding is shown in figure 2. In this figure the Bouguer gravity anomalies of the Amado subbasin and the southern end of the Tucson basin are overlain on the pattern of the Tertiary and Quaternary upper basin fill and surficial deposits mapped by Drewes (1980). The parts of the piedmont that overlie the subbasins were mapped as Quaternary gravel whereas the parts of the piedmont at the edges of the subbasins and between the two subbasins were mapped as Quaternary and Tertiary gravel. The map pattern shows the older Quaternary and Tertiary gravel to be more dissected than the Quaternary gravel. Thus, deposition apparently is occurring above the deepest part of the subbasins as indicated by the presence of Quaternary gravel, and erosion is taking place at the edges of the subbasins as indicated by the presence of dissected Quaternary and Tertiary gravel. Inspection of aerial photographs verifies that southeastern edges of the Amado and Tucson subbasins coincide with fault scarps and lineaments.

## Summary

(1) This study has identified a number of previously unrecognized faults that appear to control the shape of the subbasins and affect the course of the river. The possibility that these and other faults may also control the movement of ground water should be investigated.

(2) The reconnaissance geologic mapping of this study indicates that the Nogales Formation is more widely exposed in Sopori Wash than had been mapped previously. This has the effect of further restricting the amount of upper basin-fill sediments available to act as an aquifer in the Sopori subbasin .

(3) The tuffs interbedded with the conglomerate beds at the base of the Nogales Formation may act as impermeable barriers to ground water movement. Thus, there may be a small amount of artesian ground water locally at the bottom of the subbasins.

# Part 2. Geophysical Investigations

## Data compilation

Gravity data were compiled from the gravity library of the Defense Mapping Agency and from data acquired for the mineral-resource assessment of the Coronado National Forest (Gettings, 1996). In addition U.S. Geological Survey (USGS) personnel established 83 new stations for the current investigation; 21 in the Santa Rita Mountains, 9 in the Tumacacori Mountains, and 53 within the upper Santa Cruz basin. All data were terrain corrected and the Complete Bouguer gravity anomaly value at each station was computed using standard USGS formulae as described in Gettings (1996). The resulting gravity anomaly map is shown in plate 1. The data were compiled for digital use into a grid of values at 1-km intervals covering the study area.

Aeromagnetic data were retrieved from the National Uranium Resources Evaluation (NURE) database and comprise magnetic observations at approximately 15-m intervals at a nominal terrain clearance of 120 m. Three lines cover parts of the study area; two north-south lines and one east-west line which passes just north of the community of Amado (fig. 1). Plots of these three profiles together with those on nearby bedrock are shown in plate 2. In addition, an aeromagnetic survey of much of the area was completed in December of 1996, with east-west flight lines at a spacing of 250 m and terrain clearance of 250 m. A preliminary version of this dataset has been used to complement the above data and assist in depth estimation. The final version of this dataset is not yet available and is not included here.

## Separation of the basin gravity anomaly

The interpretation of gravity anomaly data depends on the separation of the anomaly due to the geologic bodies of interest from the observed anomaly, which is the total gravity anomaly from all sources. Numerous methods are available for this proceedure, but most are numerical methods that may or may not be geologically reasonable. The method used here follows that of Saltus and Jachens (1995), and is regarded as the best for this study because it uses the gravity anomaly field from the bedrock of the surrounding ranges to define the regional field.

Based on the assumption that the rocks exposed in the adjacent ranges are likely to be the same as those that underlie the upper Santa Cruz and Sopori basins, the regional field was defined by generating a coarse interval grid (4-km in this case) from stations that are not located on upper basin fill or on Nogales Formation. The coarse grid was then resampled at 1-km intervals to yield the regional gravity anomaly field shown in plate 3. This grid was subtracted from the observed complete Bouguer gravity anomaly grid to yield a residual gravity anomaly grid (plate 4). It is necessary to do the initial regional grid at a larger interval in order to get a smooth interpolation across the basin where there are no observations on bedrock. Because the density-

depth functions are fixed in the formulation of Saltus and Jachens (1995), whereas here the object is to find the variations in the depth to the intra-sedimentary contact, the modeling scheme is carried out somewhat differently from that described by those authors. In this study, the residual gravity anomaly, shown in plate 4, forms the basic data for analysis.

## Basin fill density functions

The second element critical to successful estimation of depths from gravity anomaly data is the assumed density of the material filling the basin and that of the bedrock below. No density data from well logs within the upper Santa Cruz basin are available so density data from wells drilled in nearby basins were used. Figure 3 shows the measured densities as a function of depth for a deep petroleum exploration well drilled in 1972 in the Tucson basin and two wells in the Avra Valley west of Tucson (Tucci and others, 1982). These densities were determined by downhole gravimeter measurements, which are the most desirable because they give a good average for a volume of the order of a thousand cubic meters about the measurement point. Although the data show large scatter, they are reasonably well fit by three straight line segments (fig. 3). The three segments correspond to density in the unsaturated sediments above water table, saturated but unconsolidated sediments below water table, and consolidated sediments that are assumed to correlate with the Nogales Formation of the upper Santa Cruz Valley. The gentle slope of the lines to higher densities with increasing depth is interpreted to be due to compaction. Figure 4 shows the downhole gravimeter data of figure 3 together with the digitized gamma-gamma formation density log of the upper 914 m (3,000 ft) of the deep petroleum exploration well in the Tucson basin (Exxon, no. 1 State (32), Schlumberger geophysical logs available at the Arizona Geological Survey, Tucson Arizona). Comparison of the values shows generally good agreement between the gamma-gamma log and the gravimeter except in the interval of 183-244 m (600-800 ft) depth. Examination of the caliper log shows that this interval has numerous large washouts and evidently the compensation factors were not adequate to correct the log in these areas. However, for parts of the log where washouts are not significant, averages of the gamma-gamma log are evidently a reliable measure of bulk density. Note that there is considerable variation in the density values below 305 m (1,000 ft); this variation may to be due to changes in the proportion of fines, sand, and gravel, as well as degree of cementation.

Grain density of cuttings from the upper 308 m of the Exxon hole was measured to allow estimates of porosity. For 27 measurements at depths from 70 m to 308 m, the mean grain density was 2.57 g/cc, with a maximum of 2.64 g/cc, a minimum of 2.38 g/cc, and a standard deviation of 0.06 g/cc.

In the course of geologic reconnaissance field work (Part 1) several sections of the Nogales Formation with relief of 30 m or more were located. In such exposures, a surface gravimetric profile can be used to calculate the bulk density of the unit, similar to borehole gravity measurements.

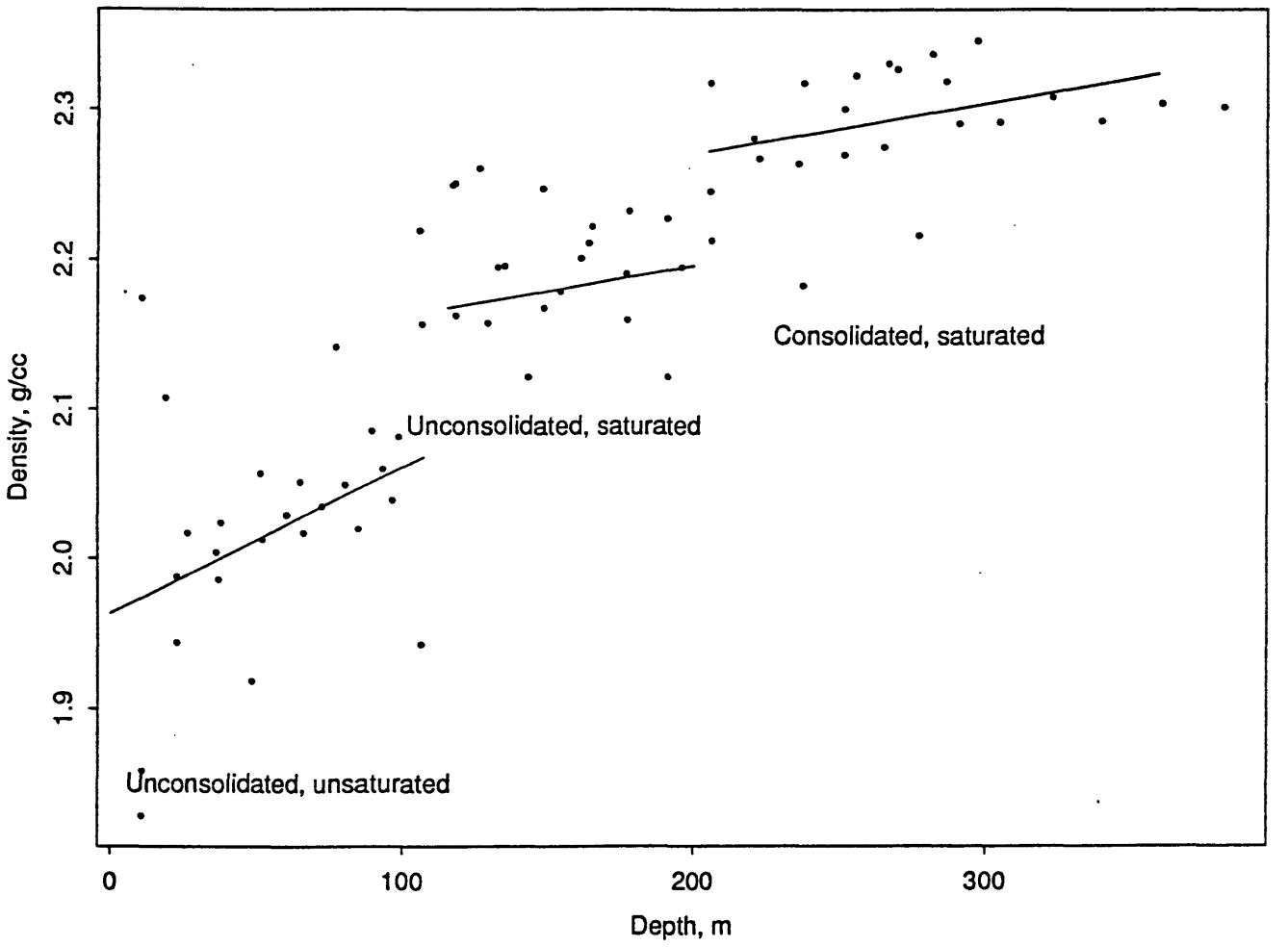


Figure 3. Bulk density as a function of depth estimated from borehole gravimeter measurements in one borehole in the Tucson basin and two boreholes in the Avra Valley immediately west of the Tucson basin (data from Tucci and others, 1982). The three line segments are least squares fits of the data points in each of the three clusters. The clusters are interpreted to be the densities of unconsolidated and unsaturated basin fill, unconsoidated and saturated basin fill, and consolidated and saturated basin fill. The consolidated and saturated fill is analogous to the Nogales Formation in the study area, and the unconsolidated fill is analogous to the upper basin fill in the study area.

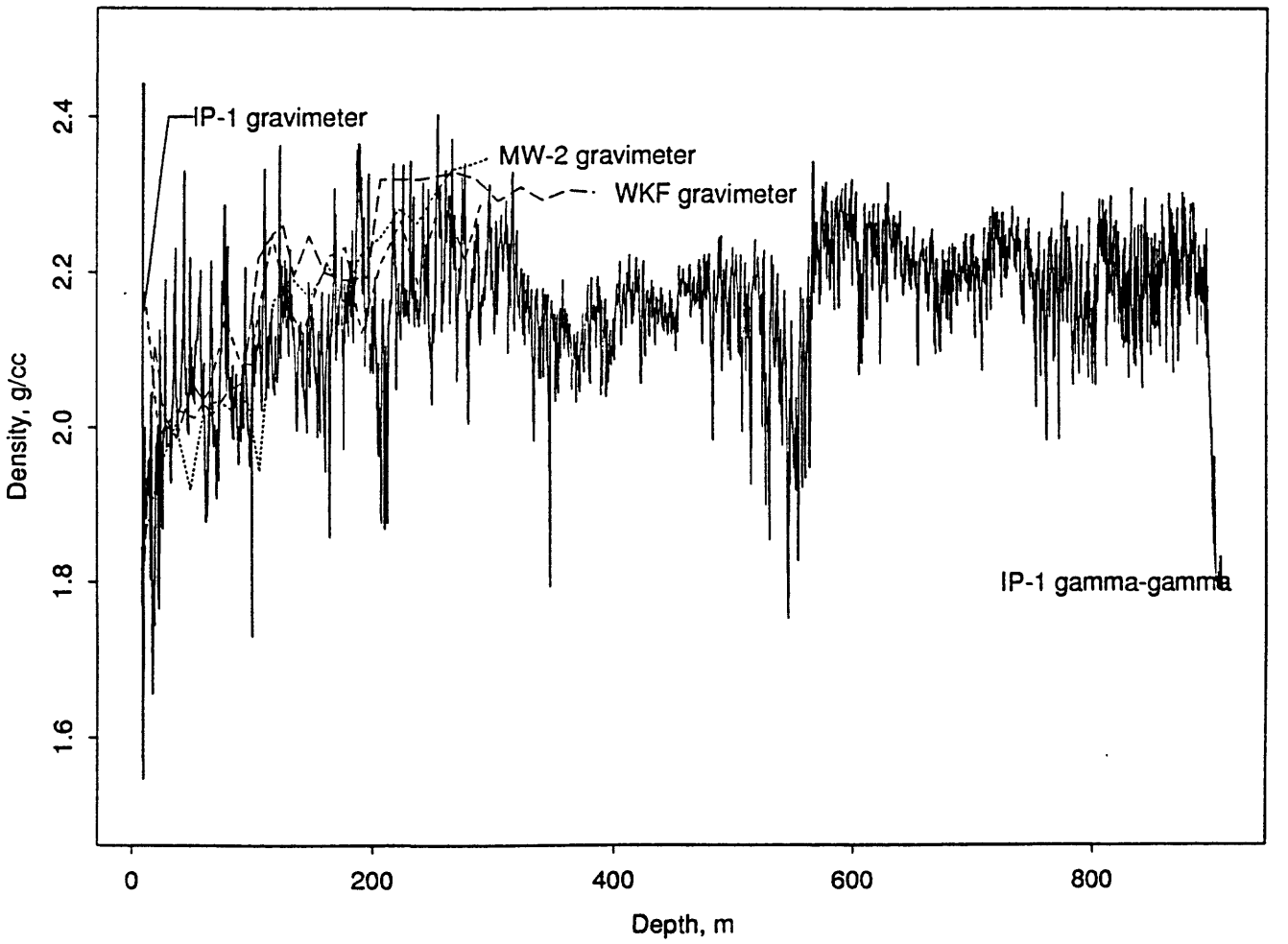


Figure 4. Bulk density logs for a borehole in the Tucson basin and two boreholes in the Avra Valley. The dotted line (MW-2 gravimeter), the dashed line (WKF gravimeter), and the solid line (IP-1 gravimeter) are data points from borehole gravimeter measurements (Tucci and others, 1982). The line labeled IP-1 gamma-gamma is a compensated gamma-gamma density log for the upper 914 m of the borehole in the Tucson basin (Electrical Log Services, Midland Texas, written communication, 1996). The only areas of significant disagreement between the gamma-gamma log and the gravimeter log of the same hole (IP-1 gravimeter line) are where the caliper log for the hole shows washouts; see text for details.

Measurements were made in the Nogales Formation at two sites in Proctor Wash northwest of Arivaca Junction, two sites in Agua Fria Canyon west of Rio Rico, and three sites in Cottonwood Canyon east of Tubac (fig. 1). Measurements of the upper basin fill were made on the Rex Ranch road east of Amado and about two miles east of Tubac. The results were reduced using the method of Parasnis (1952) and are summarized in table 2.

Table 2. Summary of in situ measurements of bulk density using gravimetric methods.
[N is number of stations in the profile. TC is terrain correction.]

| Site | Lon (deg) | Lat (deg) | N | Density (g/cc) | Comment |
|---|---|---|---|---|---|
| **Nogales Formation** | | | | | |
| Proctor Wash | 111.1937 | 31.8233 | 8 | 2.00±0.08 | |
| Proctor Wash | 111.1944 | 31.8274 | 5 | 2.00±0.02 | |
| Agua Fria Canyon | 111.0543 | 31.4270 | 11 | 2.07±0.01 | |
| Agua Fria Canyon | 111.0522 | 31.4282 | 2 | 2.16 | |
| Cottonwood Canyon | 110.9784 | 31.6372 | 3 | 2.38±0.02 | |
| Cottonwood Canyon | 110.9785 | 31.6381 | 2 | 2.08 | TC may be too small |
| Cottonwood Canyon | 110.9669 | 31.6392 | 2 | 2.38 | |
| **Upper basin fill** | | | | | |
| Rex Ranch road | 110.9980 | 31.6962 | 4 | 1.87 | |
| East of Tubac | 111.0272 | 31.6239 | 2 | 2.30 | Poor site - TC uncertain |
| **Terrace deposits** | | | | | |
| Cottonwood Canyon | 110.9784 | 31.6372 | 3 | 2.64±0.02 | Calcite cemented; limestone and mafic volcanic clasts |

For the upper basin fill, the results at the Tubac site are not considered reliable because a density of 2.30 g/cc is much higher than most values given in the literature for unconsolidated materials with similar composition, and there is no evidence in the exposures (such as magnetite sands) to suggest such a high density. The topography of this site is very complex, making a reliable terrain correction for density determination difficult. The low relief and gentle angle of the exposure all contribute to uncertainty in the measurement. This leaves only the Rex Ranch road site, which at 1.87 g/cc, falls within the range of values measured in the drillholes (fig. 4). Because of

the known large variability of densities for this unit, we chose to use the average of the dry, unconsolidated sediments from the three drillholes as the best estimate of the upper basin fill density. This value is 2.03 g/cc for the unsaturated sediments. Assuming a grain density equal to measured average of 2.57 g/cc discussed above, a porosity of 21% results. For the saturated material, this implies a density of 2.24 g/cc. These values are in reasonably good agreement with the values shown on figure 3.

For the Nogales Formation sites, a mean dry bulk density value of 2.15 g/cc was obtained for 7 sites, with a maximum value of 2.38 g/cc, a minimum value of 2.00 g/cc and a standard deviation of 0.16 g/cc. Again assuming a grain density of 2.57 g/cc from the borehole cuttings measurements an average porosity of 16% is obtained, and a saturated bulk density of 2.32 g/cc is implied. This value is also in good agreement with the borehole observations on figure 3. We have thus concluded that the borehole data of figure 3, supplemented by the surface measurements, give reliable estimates of the basin fill densities.

Density functions which are a function of depth present analytical difficulties in gravity anomaly model calculations, so the three line segments of figure 3 are approximated with constant mean values for intervals as tabulated in table 3 and shown in figure 5. Note that more intervals are used in the shallow part of the function where the density changes with depth are large. The shallow layers also have a larger effect because gravity varies as the inverse square of distance, so it is important to model them adequately. The functions plotted in figure 5 are the density contrasts, that is, the difference between the sediment density and the bedrock density, because only the contrast is important in the model calculations. Considering the likely composition of the bedrock based on the geologic map of Drewes (1980) shown in figure 2, 2.65 g/cc was chosen as the average density for bedrock. If the rhyolitic rocks of the Tumacacori Mountains underlie large areas of the basin, this value may be too large and the density contrasts should be smaller. If this is the case, the depth estimates will be too shallow because more sediments would be necessary to create the observed mass deficiency of the gravity anomaly.

In table 3 and figure 5, the depth to the water table has been taken as 46 m (150 ft), the average depth to water in wells used in this study (table 4). Note that there is a large change in the density contrast at the water table so that it is important to include the unsaturated sediments in the gravity model if the depth to water is substantial. For a 50 m depth to water and the upper basin fill density contrast of figure 5, modeling the dry sediments as saturated would result in an error of about 0.5 mgal, which could change depth estimates significantly.

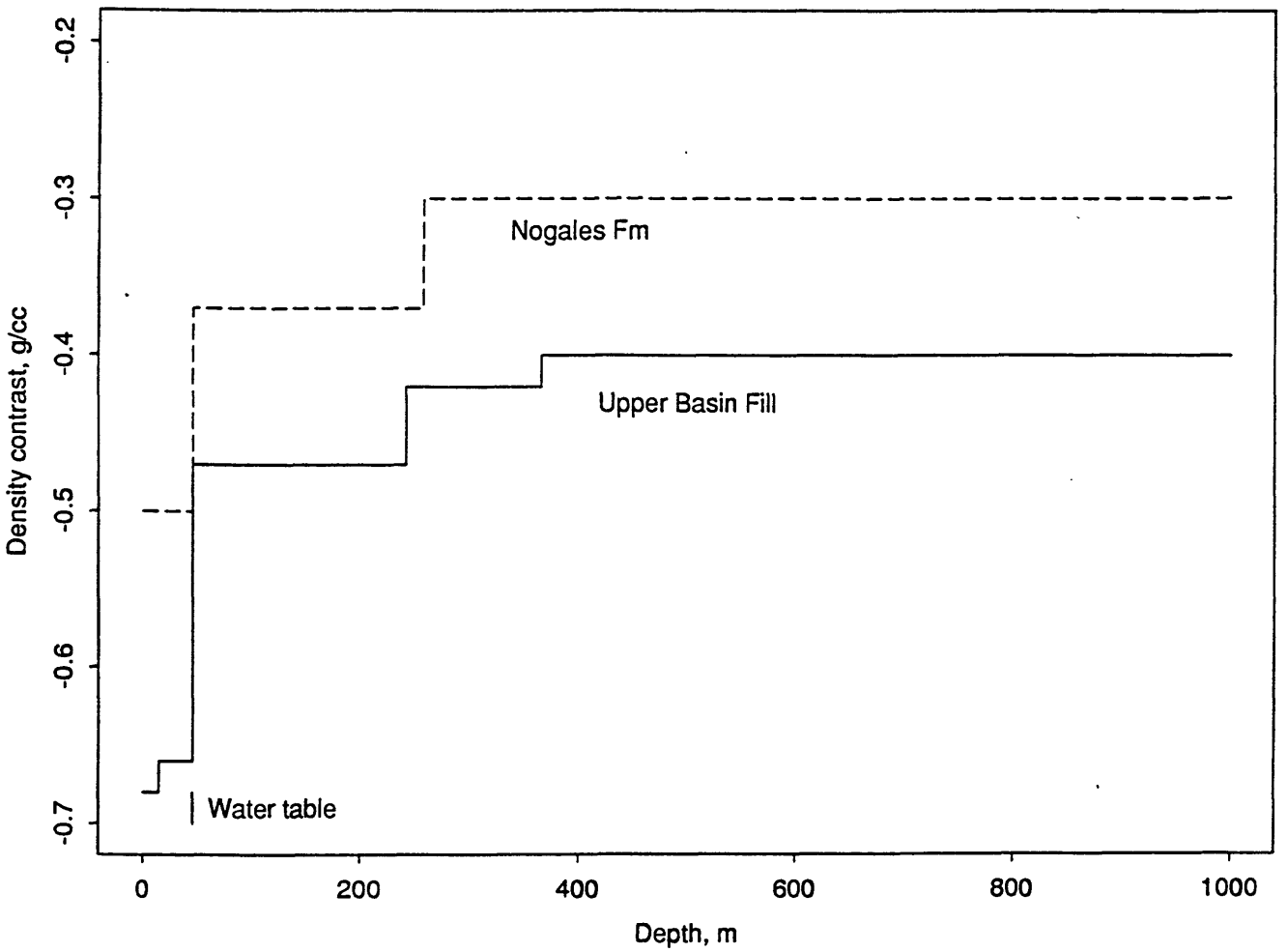


Figure 5. Density contrast functions adopted for the upper Santa Cruz Valley study area. The function labeled Nogales Fm represents the density contrast between the lower basin fill (Nogales Formation) and bedrock beneath the basin; the function labeled Upper Basin Fill represents the density contrast between the upper basin fill unit and bedrock beneath the basin.

Table 3. Density versus depth functions for the upper basin fill and Nogales Formation (see text for details).
[Density contrast is sediment density minus bedrock density.]

| Unit | Depth (ft) | Depth (m) | Density (g/cc) | Density contrast (g/cc) |
|---|---|---|---|---|
| **Upper basin fill** | | | | |
| dry | 0-50 | 0-15 | 1.97 | -0.68 |
| dry | 50-150 | 15-46 | 1.99 | -0.66 |
| saturated | 150-790 | 46-241 | 2.18 | -0.47 |
| saturated | 790-1200 | 241-366 | 2.23 | -0.42 |
| saturated | 1200 | 366 | 2.25 | -0.40 |
| **Nogales Formation** | | | | |
| dry | 0-150 | 0-46 | 2.15 | -0.50 |
| saturated | 150-690 | 46-256 | 2.28 | -0.37 |
| saturated | 690 | 256 | 2.35 | -0.30 |
| **Bedrock** (estimated) | | | 2.65 | |

## Drillhole information

Drillers' logs of water wells were studied for information on depth to bedrock and thickness of upper basin fill. Table 4 gives the results of these studies for 97 selected wells. Forty-three wells from tables 4 and 5 and two drillholes shown on plate 5 (about 3.5 km southwest of latitude 32 deg. 45min., longitude 111 deg., and just east of Diablito Mtn) were interpreted as having penetrated the Nogales Formation and were used as primary points for estimating depths to the base of the Nogales Formation as described below. The locations of these 45 wells are shown on plate 5.

Table 4. Drillers' logs of water wells, upper Santa Cruz Valley with interpretation of geologic units that were penetrated. All depths and elevations are in feet. See appendix for explanation of well location system used in Arizona.
[ubf = upper basin fill; Nogales = Nogales Formation]

| Well no. | Location | Quadrangle | Collar elev. | TD | Depth to water | Interval | Lithology |
|---|---|---|---|---|---|---|---|
| 1 | D(19-11)1bbd | Batamote Hills | 3925 | 400 | 142 | 0-90<br>90-400 | ubf<br>Nogales |

| | | | | | | | |
|---|---|---|---|---|---|---|---|
| 2 | D(18-13)21ccc | Esperanza Mill | 3135 | 956 | 298 | 0-550<br>550-800<br>800-956 | ubf<br>Nogales<br>rock chips |
| 3 | D(18-13)28bbb | Esperanza Mill | 3134 | 960 | 325 (?) | 0-950<br>950-960 | ubf?<br>limestone bedrock |
| 4 | D(18-13)28cbb | Esperanza Mill | 3122 | 1100 | 325 (?) | 0-1070<br>1070-1100 | ubf?<br>rhyolite bedrock |
| 5 | D(18-13)28ccc | Esperanza Mill | 3096 | 1038 | 908 (?) | 0-1032<br>1032-1038 | ubf?<br>siltstone bedrock |
| 6 | D(18-13)28ccc | Esperanza Mill | 3098 | 1035 | 270 (?) | 0-500<br>500-925<br>925-1035 | ubf<br>Nogales?<br>rock |
| 7 | D(18-13)29ddc | Esperanza Mill | 3092 | 1065 | 305 (?) | 0-1030<br>1030-1065 | ubf?<br>andesite bedrock |
| 8 | D(19-13)3acc | Esperanza Mill | 2915 | 234 | 40 | 0-195<br>195-234 | old well<br>ubf |
| 9 | D(19-13)5abb | Esperanza Mill | 3070 | 350 | 208 (?) | 0-265<br>265-350 | ubf<br>ubf, cemented |
| 10 | D(19-13)5acb | Esperanza Mill | 3070 | 351 | 235 (?) | 0-351 | ubf |
| 11 | D(19-13)5cdd | Esperanza Mill | 3120 | 363 | 252 (?) | 0-363 | ubf |
| 12 | D(19-13)7dda | Esperanza Mill | 3120 | 355 | 120 (?) | 0-355 | ubf |
| 13 | D(19-13)bbc | Esperanza Mill | 3150 | 382 | 240 (?) | 0-382 | ubf |
| 14 | D(19-13)9acc | Esperanza Mill | 2940 | 400 | 125 (?) | 0-230<br>230-400 | old well<br>ubf |
| 15 | D(19-13)9dbb | Esperanza Mill | 2940 | 257 | 60 | 0-257 | ubf |
| 16 | D(19-13)10bcb | Esperanza Mill | 2938 | 793 | 49 (?) | 0-755<br>755-793 | ubf<br>Nogales?, conglomerate |
| 17 | D(19-13)16bad | Esperanza Mill | 2953 | 811 | 54 (?) | 0-785<br>785-813 | ubf<br>Nogales?, large rocks |

| | | | | | | | |
|---|---|---|---|---|---|---|---|
| 18 | D(19-13)17bab | Esperanza Mill | 3060 | 350 | 280 | 0-300<br>300-350 | ubf<br>ubf?, conglomerate |
| 19 | D(19-13)21ccc | Esperanza Mill | 2990 | 250 | 34 (?) | 0-250 | ubf |
| 20 | D(18-13)26aad | Green Valley | 2870 | 269 | 40 | 0-269 | ubf |
| 21 | D(18-13)26dbd | Green Valley | 2890 | 1200 | (?) | 0-1200 | ubf |
| 22 | D(18-13)27daa | Green Valley | 2890 | 1300 | (?) | 0-828<br>828-1300 | ubf<br>Nogales?, cemented |
| 23 | D(18-13)35cba | Green Valley | 2895 | 1000 | 60 | 0-1000 | ubf |
| 24 | D(18-14)19ccd | Green Valley | 3010 | 505 | 265 | 0-505 | ubf |
| 25 | D(19-13)3 adc | Green Valley | 2917 | 1200 | (?) | 0-1200 | ubf |
| 26 | D(19-13)22aad | Green Valley | 3100 | 400 | 240 | 0-400 | ubf |
| 27 | D(19-13)22dbc | Green Valley | 3105 | 340 | 210 | 0-340 | ubf |
| 28 | D(19-13)22dcc | Green Valley | 3125 | 310 | 210 | 0-310 | ubf |
| 29 | D(19-13)23bcc | Green Valley | 2990 | 310 | 220 | 0-310 | ubf |
| 30 | D(20-11)20ddc | Saucito Mt | 3580 | 220 | 100 | 0-20<br>20-220 | ubf<br>Nogales, cemented |
| 31 | D(20-11)21cac | Saucito Mt | 3530 | 415 | 73 | 0-40<br>40-415 | ubf<br>Nogales, gray rock |
| 32 | D(20-11)21cda | Saucito Mt | 3500 | 300 | 115 | 0-10<br>10-300 | ubf<br>Nogales, cemented |
| 33 | D(20-11)28aaa | Saucito Mt | 3450 | 220 | 30 | 0-5<br>5-220 | ubf<br>Nogales, cemented conglomerate |
| 34 | D(20-11)28bac | Saucito Mt | 3478 | 500 | 30 | 0-6<br>6-500 | ubf<br>Nogales, cemented conglomerate |

| | | | | | | | |
|---|---|---|---|---|---|---|---|
| 35 | D(20-11)29abc | Saucito Mt | 3530 | 480 | 450 | 0-450<br>450-480 | Nogales<br>andesite bedrock |
| 36 | D(20-11)29adc | Saucito Mt | 3580 | 284 | 52 | 0-8<br>8-276<br>276-284 | ubf<br>Nogales, cemented<br>solid rock |
| 37 | D(20-11)32dac | Saucito Mt | 3530 | 280 | 32 | 0-30<br>30-280 | ubf<br>Nogales,<br>conglomerate |
| 38 | D(20-11)32ddc | Saucito Mt | 3540 | 400 | 40 | 0-400 | ? (cement not mentioned) |
| 39 | D(19-12)36caa | Amado | 3118 | 230 | 141 | 0-180<br>180-230 | ubf<br>Nogales?,<br>cemented |
| 40 | D(19-12)36cac | Amado | 3120 | 220 | 149 | 0-220 | ubf |
| 41 | D(19-12)36cad | Amado | 3122 | 240 | 140 | 0-185<br>185-240 | ubf<br>Nogales?,<br>cemented |
| 42 | D(19-12)36cbb | Amado | 3143 | 230 | 164 | 0-230 | ubf |
| 43 | D(19-12)36cbd | Amado | 3130 | 240 | 151 | 0-240 | ubf |
| 44 | D(19-12)36cca | Amado | 3130 | 240 | 160 | 0-182<br>182-240 | ubf<br>Nogales?,<br>cemented |
| 45 | D(19-12)36cca | Amado | 3130 | 240 | 180 | 0-180<br>180-240 | ubf<br>Nogales?,<br>cemented |
| 46 | D(19-12)36ccd | Amado | 3135 | 240 | 147 | 0-240 | ubf |
| 47 | D(1912)36cdc | Amado | 3125 | 250 | 170 | 0-220<br>220-250 | ubf<br>Nogales?,<br>cemented |
| 48 | D(19-12)36ddc | Amado | 3090 | 307 | 88 or 105 | 0-307 | ubf |
| 49 | D19-13)29ccc | Amado | 3015 | 301 | 36 (?) | 0-301 | ubf |
| 50 | D(19-13)29ddb | Amado | 3030 | 410 | 62 | 0-410 | ubf |
| 51 | D(19-13)31adc | Amado | 3033 | 204 | 60 | 0-70<br>70-204 | ubf<br>Nogales?,<br>cemented |

| | | | | | | | |
|---|---|---|---|---|---|---|---|
| 52 | D(1913)31ccc | Amado | 3070 | 260 | 58 | 0-75<br>75-260 | ubf<br>Nogales?, cemented conglomerate |
| 53 | D(20-12)3ddd | Amado | 3200 | 450 | 148 or 168 | 0-450 | ubf |
| 54 | D(20-13)19ccb | Amado | 3124 | 220 | 40 | 0-220 | ubf |
| 55 | D(20-13)29bbb | Amado | 3150 | 260 | 155 (?) | 0-260 | ubf |
| 56 | D(20-13)32bac | Amado | 3170 | 203 | 68 | 0-203 | ubf |
| 57 | D(20-13)32aac | Amado | 3300 | 275 | 191 | 0-275 | ubf |
| 58 | D(20-13)32aca | Amado | 3290 | 270 | 190 | 0-53<br>53-270 | ubf<br>Nogales?, cemented |
| 59 | D(20-13)33bcd | Amado | 3290 | 290 | 160 | 0-192<br>192-290 | ubf<br>Nogales?, cemented |
| 60 | D(21-13)4abc | Amado | 3390 | 530 | 172 | 0-510<br>510-530 | ubf<br>Nogales, tight conglomerate |
| 61 | D(21-13)4dcc | Amado | 3330 | 500 | 147 | 0-320<br>320-505 | ubf<br>Nogales?, conglomerate |
| 62 | D(21-13)6bbc | Amado | 3240 | 203 | 110 | 0-203 | ubf |
| 63 | D(21-13)6daa | Amado | 3175 | 300 | 36 | 0-100<br>100-300 | ubf<br>Nogales?, hard cement |
| 64 | D(20-13)13dad | Mt Hopkins | 3940 | 355 | 7 | 0-355 | bedrock |
| 65 | D(20-13)36ccb | Mt Hopkins | 3717 | 300 | (?) | 0-300 | Nogales, conglomerate, and rock |
| 66 | D(21-11)5dcd | Murphy Peak | 3600 | 300 | 31 | 0-300 | ubf |
| 67 | D(21-11)20ada | Murphy Peak | 3720 | 300 | (?) | 0-300 | volcanic bedrock |
| 68 | D(21-12)12aab | Tubac | 3345 | 300 | 178 | 0-235<br>235-300 | ubf<br>Nogales?, cemented |

| | | | | | | | |
|---|---|---|---|---|---|---|---|
| 69 | D(21-12)13aca | Tubac | 3365 | 360 | 225 | 0-180<br>180-360 | ubf<br>Nogales, sandstone |
| 70 | D(21-12)23add | Tubac | 3700 | 1000 | 490 | 0-470<br>470-650<br>650-1000 | ubf<br>Nogales, sandstone<br>granite bedrock |
| 71 | D(21-12)24aaa | Tubac | 3380 | 512 | 155 | 0-487<br>487-519 | ubf<br>red bedrock |
| 72 | D(21-13)7caa | Tubac | 3242 | 651 | 73 | 0-335<br>335-660 | ubf<br>Nogales, red and gray rock |
| 73 | D(21-13)18cbc | Tubac | 3320 | 240 | 147 | 0-160<br>160-240 | ubf<br>Nogales, cemented |
| 74 | D(21-13)18aaa | Tubac | 3203 | 220 | 132 | 0-220 | ubf |
| 75 | D(21-13)18cad | Tubac | 3340 | 230 | 130 | 0-230 | ubf |
| 76 | D(21-13)19bba | Tubac | 3320 | 220 | 126 | 0-175<br>175-220 | ubf<br>Nogales, cemented |
| 77 | D(21-13)19bbb | Tubac | 3365 | 240 | 165 | 0-190<br>190-240 | ubf<br>Nogales, cemented |
| 78 | D(21-13)20bac | Tubac | 3215 | 560 | 325 | 0-420<br>420-560 | ubf<br>Nogales, cemented |
| 79 | D(21-13)21adb | Tubac | 3540 | 540 | 358 | 0-130<br>130-540 | ubf<br>Nogales, cemented |
| 80 | D(22-13)7dcc | Tubac | 3690 | 520 | 405 | 0-520 | ubf |
| 81 | D(22-13)8caa | Tubac | 3598 | 450 | 365 (?) | 0-450 | ubf |
| 82 | D(21-13)13bda | San Cayetano | 3800 | 600 | 449 | 0-17<br>17-600 | ubf<br>Nogales, sandstone |
| 83 | D(21-13)23acb | San Cayetano | 3740 | 700 | 465 | 0-130<br>130-700 | ubf<br>Nogales, cemented conglomerate |
| 84 | D(22-13)19dcc | Pena Blanca L. | 3523 | 300 | 191 | 0-210<br>210-300 | ubf<br>Nogales, cemented |
| 85 | D(23-13)4ddd | Pena Blanca L. | 3683 | 280 | 115 | 0-160<br>160-280 | old well<br>Nogales, cemented |

| | | | | | | | |
|---|---|---|---|---|---|---|---|
| 86 | D(23-13)18 | Pena Blanca L. | 3640 | 300 | 12 | 0-35<br>35-300 | Nogales tuff, rock, and conglomerate |
| 87 | D(23-13)29ccc | Pena Blanca L. | 3960 | 550 | 250 | 0-550 | ubf |
| 88 | D(23-12)36bcd | Pena Blanca L. | 4015 | 400 | 5 | 0-40<br>40-400 | Nogales tuff |
| 89 | D(23-13)1dbb | Rio Rico | 3445 | 260 | 43 | 0-80<br>80-260 | ubf<br>Nogales, conglomerate |
| 90 | D(23-13)25aba | Rio Rico | 3600 | 400 | 27 | 0-400 | ubf |
| 91 | D(23-13)25bdd | Rio Rico | 3635 | 250 | 58 | 0-250 | ubf |
| 92 | D(23-13)36aad | Rio Rico | 3680 | 320 | 144 | 0-220<br>220-320 | ubf<br>Nogales, cemented |
| 93 | D(23-13)36adb | Rio Rico | 3675 | 400 | 100 (?) | 0-400 | ubf |
| 94 | D(23-13)36bdd | Rio Rico | 3717 | 310 | 129 | 0-170<br>170-310 | ubf<br>Nogales, cemented |
| 95 | D(23-13)36dbb | Rio Rico | 3705 | 450 | 130 | 0-195<br>195-450 | ubf<br>Nogales?, cemented |
| 96 | D(23-14)17ccc | Rio Rico | 3685 | 310 | 100 | 0-310 | granite, volcanics |
| 97 | D(23-14)18ddb | Rio Rico | 3710 | 360 | 123 | 0-360 | granite |

Table 5. Data for 45 boreholes used to estimate depth to bedrock.
[Well nos. are those in table 4. Unnumbered well locations are shown on plates 6 and 7. TD is total depth. Rs and Rd are the radius of shallow and deep cylinders models used to estimate depth to bedrock.]

| Well no. | Residual gravity anomaly (mGals) | Depth to water (km) | Depth to No-gales (km) | TD (km) | Rs (km) | Rd (km) | Lon (degrees) | Lat (degrees) | Calculated depth to bedrock (km) |
|---|---|---|---|---|---|---|---|---|---|
| BH1 | 12.1 | .018 | .259 | 0.274 | 7 | 3.5 | 111.03020 | 31.73590 | 0.920 |
| BH2 | 5.3 | .012 | .174 | 0.198 | 3 | 1.0 | 110.97820 | 31.47110 | 0.350 |
| 1 | 4.2 | .043 | .027 | 0.122 | 3 | 3.0 | 111.17724 | 31.80998 | 0.260 |
| 16[1] | 3.0 | .015 | .230 | 0.242 | 6 | 2.0 | 111.00943 | 31.79476 | 0.150 |
| 17 | 5.7 | .016 | .239 | 0.247 | 6 | 2.0 | 111.01907 | 31.78203 | 0.330 |
| 30 | 1.8 | .030 | .006 | 0.067 | 3 | 3.0 | 111.23471 | 31.66871 | 0.100 |

| | | | | | | | | | |
|---|---|---|---|---|---|---|---|---|---|
| 31 | 2.5 | .022 | .012 | 0.126 | 3 | 3.0 | 111.22617 | 31.67190 | 0.150 |
| 32 | 2.5 | .035 | .003 | 0.091 | 3 | 3.0 | 111.22409 | 31.67039 | 0.150 |
| 33 | 3.5 | .009 | .002 | 0.067 | 3 | 3.0 | 111.21551 | 31.66672 | 0.130 |
| 34 | 2.0 | .009 | .002 | 0.152 | 3 | 3.0 | 111.22606 | 31.66485 | 0.130 |
| 35[2] | 1.5 | .137 | .000 | 0.146 | 3 | 3.0 | 111.23875 | 31.66487 | 0.075 |
| 36[3] | 1.6 | .016 | .002 | 0.087 | 3 | 3.0 | 111.23465 | 31.66128 | 0.100 |
| 37 | 2.4 | .010 | .009 | 0.085 | 3 | 3.0 | 111.23455 | 31.64295 | 0.150 |
| 39 | 8.5 | .043 | .055 | 0.070 | 5 | 3.0 | 111.07061 | 31.67496 | 0.640 |
| 41 | 7.0 | ,043 | .056 | 0.073 | 5 | 3.0 | 111.07060 | 31.68060 | 0.500 |
| 44 | 2.6 | .049 | .055 | 0.073 | 5 | 2.0 | 111.07489 | 31.66090 | 0.135 |
| 45 | 2.6 | .055 | .055 | 0.073 | 5 | 2.0 | 111.07421 | 31.65972 | 0.130 |
| 47 | 3.0 | .052 | .067 | 0.076 | 5 | 2.0 | 111.07275 | 31.65995 | 0.154 |
| 51 | 13.3 | .018 | .021 | 0.062 | 7 | 4.0 | 111.04737 | 31.73308 | 1.140 |
| 52 | 11.6 | .018 | .023 | 0.079 | 5 | 3.0 | 111.05870 | 31.68874 | 1.010 |
| 58 | 7.8 | .058 | .016 | 0.082 | 5 | 3.0 | 111.03133 | 31.50903 | 0.590 |
| 59 | 5.8 | .049 | .058 | 0.088 | 5 | 3.0 | 111.02306 | 31.52015 | 0.375 |
| 60 | 7.1 | .052 | .155 | 0.162 | 5 | 3.0 | 111.01710 | 31.49932 | 0.455 |
| 61 | 6.9 | .045 | .098 | 0.152 | 6 | 3.0 | 111.01701 | 31.46684 | 0.460 |
| 63 | 6.2 | .011 | .031 | 0.091 | 6 | 4.0 | 111.04457 | 31.42483 | 0.445 |
| 65 | 2.3 | .046 | .000 | 0.091 | 1 | 0.5 | 111.97440 | 31.64162 | 0.160 |
| 67 | 5.5 | .046 | .000 | 0.091 | 3 | 3.0 | 111.23287 | 31.58959 | 0.390 |
| 68 | 2.5 | .054 | .072 | 0.091 | 4 | 2.0 | 111.06341 | 31.62245 | 0.120 |
| 69 | 2.5 | .069 | .055 | 0.110 | 4 | 4.0 | 111.06599 | 31.60439 | 0.120 |
| 70[1] | 1.1 | .149 | .143 | 0.305 | 3 | 3.0 | 111.07825 | 31.58801 | 0.030 |
| 71 | 3.8 | .047 | .148 | 0.156 | 5 | 3.0 | 111.06156 | 31.59322 | 0.170 |
| 72 | 5.3 | .022 | .102 | 0.198 | 5 | 3.0 | 111.05280 | 31.61541 | 0.340 |
| 73 | 4.1 | .045 | .049 | 0.073 | 5 | 3.0 | 111.05953 | 31.59923 | 0.235 |
| 77 | 4.5 | .050 | .058 | 0.073 | 5 | 3.0 | 111.05924 | 31.59370 | 0.260 |
| 78 | 9.5 | .099 | .128 | 0.171 | 5 | 3.0 | 111.03778 | 31.59227 | 0.680 |
| 79 | 9.7 | .109 | .040 | 0.165 | 5 | 3.0 | 111.01254 | 31.59069 | 0.730 |
| 82[4] | 2.9 | .137 | .005 | 0.183 | 2 | 2.0 | 110.96835 | 31.60669 | 0.150 |
| 83 | 8.0 | .142 | .040 | 0.213 | 5 | 2.0 | 110.98250 | 31.59131 | 0.580 |
| 84 | 4.7 | .058 | .064 | 0.091 | 4 | 2.0 | 111.05110 | 31.49381 | 0.280 |
| 86 | 4.2 | .004 | .000 | 0.091 | 4 | 3.0 | 111.05464 | 31.42776 | 0.290 |
| 89[1] | 1.2 | .013 | .024 | 0.079 | 3 | 2.0 | 110.96651 | 31.45611 | 0.065 |
| 92 | 6.1 | .044 | .067 | 0.098 | 6 | 4.0 | 110.96032 | 31.38935 | 0.400 |
| 94 | 9.3 | .039 | .052 | 0.137 | 6 | 4.0 | 110.96916 | 31.38547 | 0.700 |
| 95 | 9.0 | .040 | .059 | 0.110 | 6 | 4.0 | 110.96674 | 31.38378 | 0.670 |

1 Regional and residual anomalies poorly separated

2 No stations nearby; bedrock 138 m

3 No stations nearby; bedrock 84 m

4 No stations nearby

## Estimation of depth to bedrock

Using the density contrast functions discussed above, depths to bedrock were estimated for the wells in which the depth to Nogales Formation was known. Depths are traditionally computed using an infinite horizontal slab model for the various density layers (for example, see Litinsky, 1989) because of computational simplicity. However, the infinite slab formula is independent of depth to the slab and has infinite mass, leading to depth estimates that are too shallow. With the ready availability of computers, finite models are easily used to produce more realistic estimates. For this work, the finite right circular cylinder with vertical axis was used. For points on the axis, the exact solution is available (Duska, 1958). The model then consists of a stack of cylinders with coincident axes, each with a density contrast and thickness corresponding to the density contrast functions of figure 5 and a radius appropriate for the basin being modeled. For this work the upper basin fill or the Nogales Formation functions were used as required by the log of the well and adjusted for the depth to water table. Table 5 summarizes the parameters and the final estimated depth to bedrock for the 45 wells located on plate 5.

Next, a grid of bedrock depth estimates at a 1-km interval was computed using the following three grids as controls. (1) A grid was constructed that contained the outline of bedrock outcrop and that flagged all grid cells on bedrock as zero depth. Into this grid were inserted the locations and control depth points from the 45 wells of table 5. (2) A second grid was constructed by minimum curvature interpolation using the bedrock outcrop and the depths to the top of the Nogales Formation from the wells of table 5 as data points. This grid is the first estimate of the thickness of upper basin fill. (3) The residual gravity anomaly grid of plate 4 was used to compute depth estimates using the stack-of-cylinders model and using the second grid for the depth to the Nogales Formation and the first grid for control points. A uniform depth to water table of 46 m (150 ft) was assumed, the average value from the wells listed in table 5. The depth-to-bedrock grid is shown in plate 5 at a contour interval of 100 m.

Depth estimates calculated from the aeromagnetic anomaly profiles are shown in figures 6, 7, and 8. Because depth estimates from magnetic anomalies can be highly variable, the most reliable procedure is to use several methods and look for clusters of depth estimates. Depths from the shallow clusters in figure 6 are too shallow compared with the depths from gravity estimates in wells 70-77 (pl. 5), which are near the flight line. Farther south on the flight line, there are exposures of basalt flows interbedded with the Nogales Formation (pl. 2 and fig. 2); thus, a possible explanation for the shallow depths to bedrock indicated by the magnetic data is that they reflect similar flows in the area of the wells. In any event, the deeper clusters do give depths in agreement with the gravity estimates and have been used to help constrain the depth to bedrock. Preliminary data have been obtained from a detailed aeromagnetic survey flown in 1966 that included this study area. The image of the grid of the new data shows that the magnetic anomaly

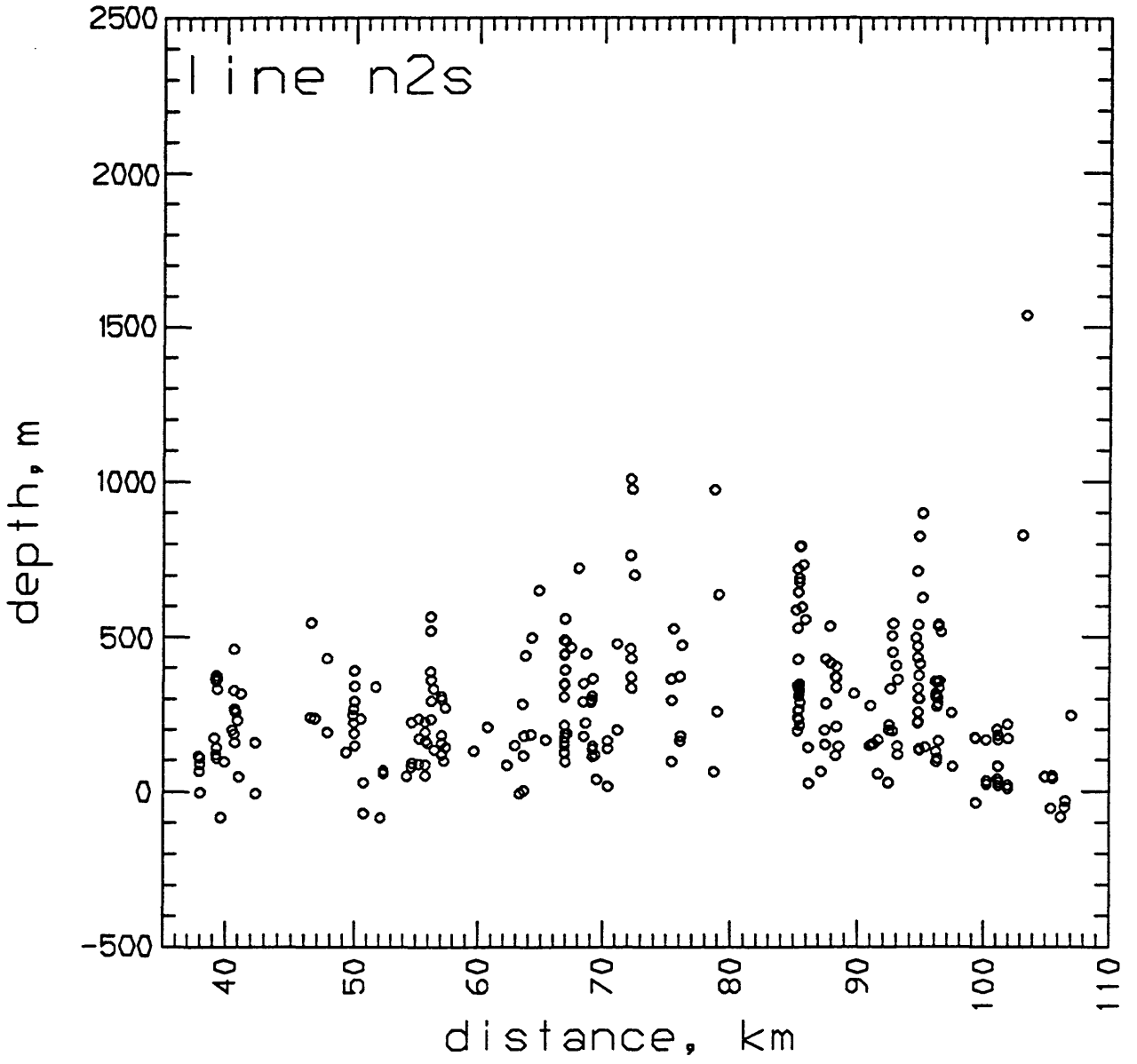


Figure 6. Depths to magnetic sources computed for National Uranium Resources Evaluation (NURE) aeromagnetic profile n2s (location on plate 2), flown north-south over the western part of the upper Santa Cruz Valley. See text for discussion.

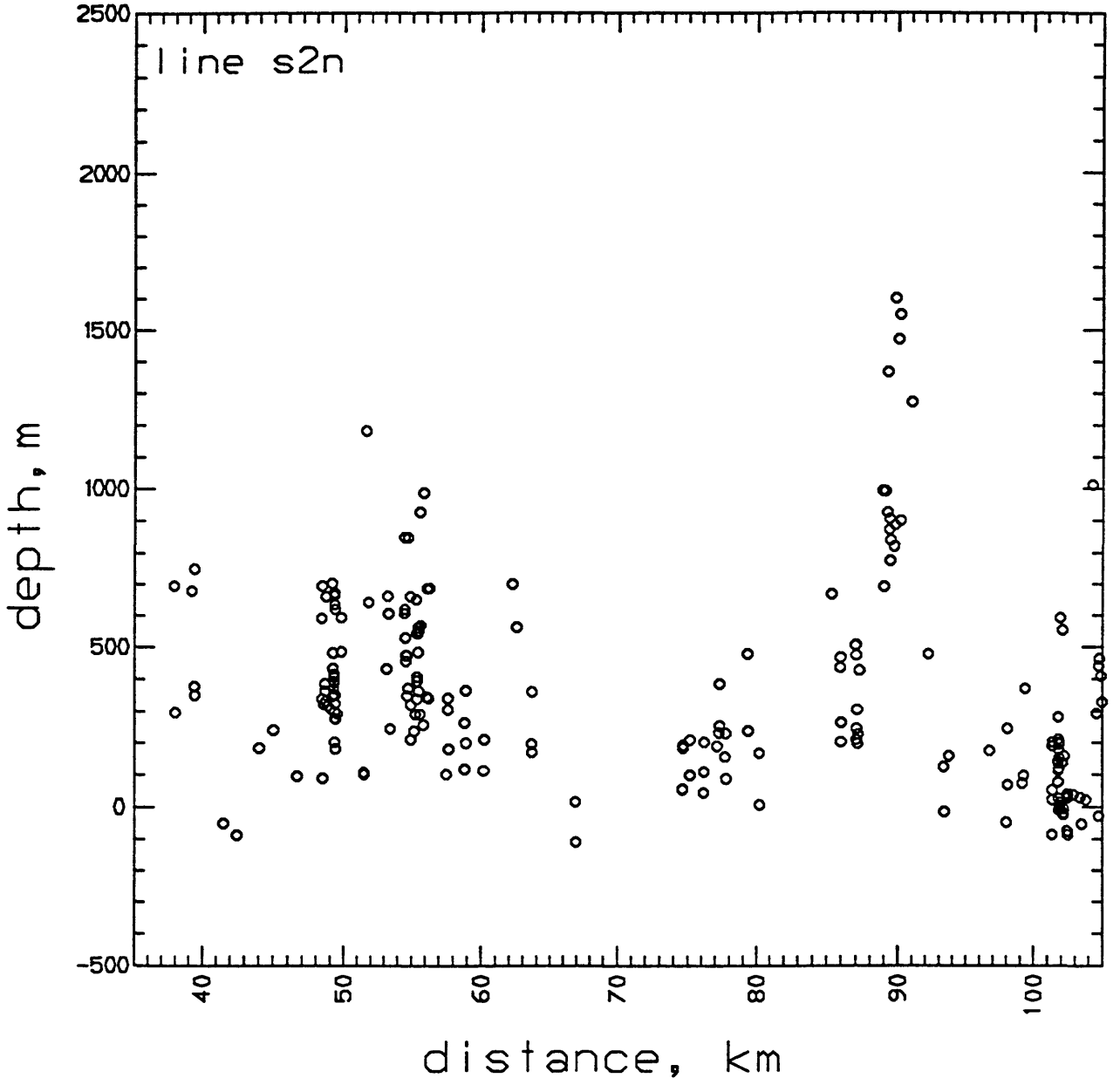


Figure 7. Depths to magnetic sources computed for NURE aeromagnetic profile s2n (location on plate 2), flown south-north over the eastern part of the upper Santa Cruz Valley. See text for discussion.

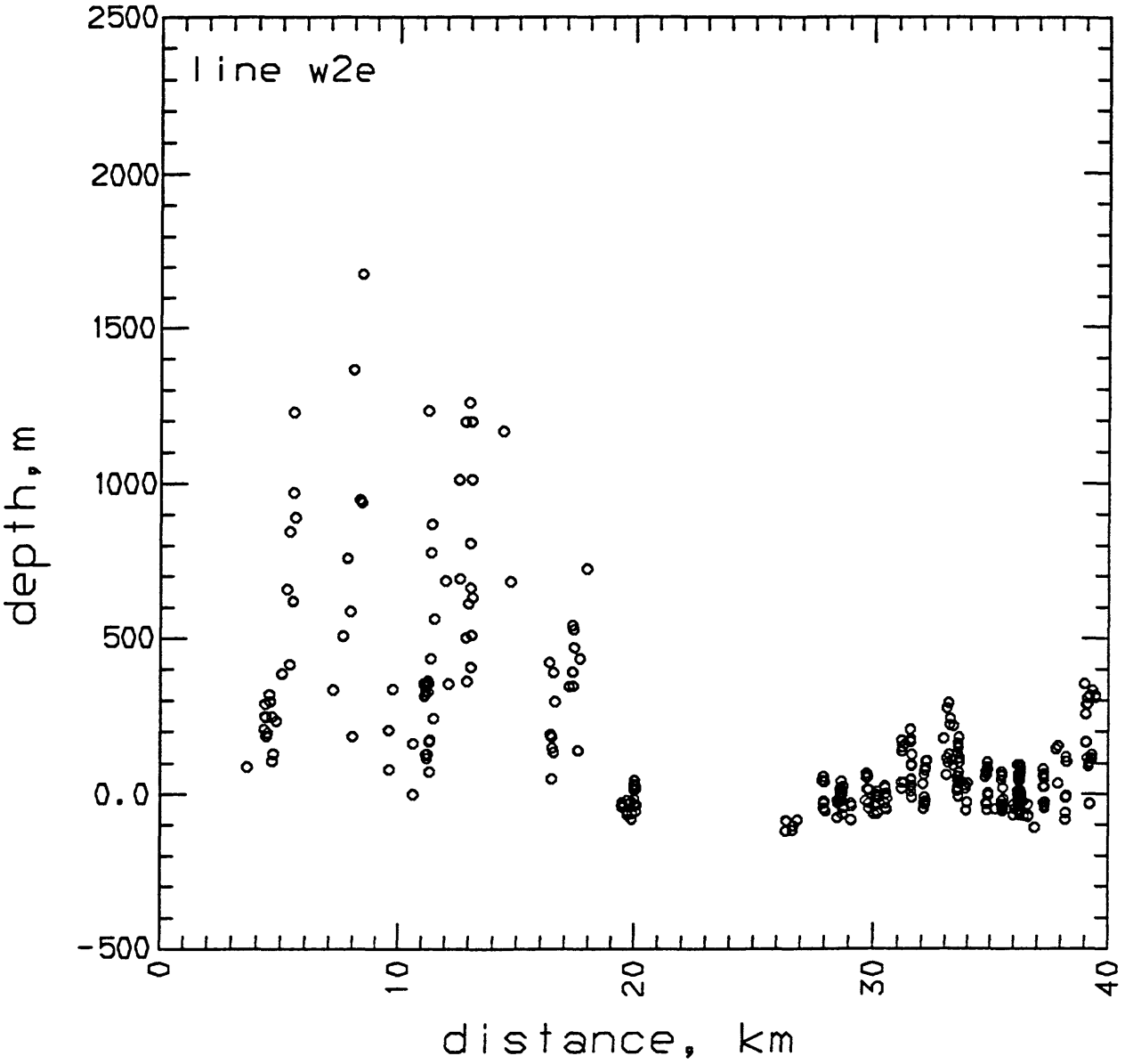


Figure 8. Depths to magnetic sources computed for NURE aeromagnetic profile w2e (location on plate 2), flown west-east over the northern part of the upper Santa Cruz Valley. See text for discussion.

data contain a great deal of information on depth and kind of bedrock beneath the basin.

## Estimation of thickness of upper basin fill

Depth to the contact between the upper basin fill and the Nogales Formation was computed from the the residual gravity anomaly (pl. 4), the estimated depth to bedrock (pl. 5), and the density contrast-depth functions of figure 5 using the following algorithm. First, the density contrast-depth function was split into one function for the upper basin fill, and a second function for the Nogales Formation. For a given total depth (depth to bedrock), one can compute the gravity anomaly as a function of the depth to the contact between the upper basin fill and the Nogales Formation. Then for the residual basin anomaly at that point, one can interpolate the depth to the contact from the gravity anomaly-depth function just computed. This proceeds for all points in the grid. Points on bedrock are not computed, and points where depths to bedrock or Nogales Formation are known (for example, wells in table 5) are not allowed to change. The model gravity effect from the new model is then computed and compared to the residual gravity anomaly grid. Differences between the model and the gravity anomaly data are then used to assess the quality of the gravity model.

Thus, this procedure finds the depth to Nogales Formation that best fits both the gravity anomaly and the estimated depth-to-bedrock datasets, constrained by the known depths to the Nogales Formation. It must be noted that because of the inherent ambiguity of solutions to the gravity anomaly field, iteration has to be used with caution, and the process is more one of interpolation of the known depths using the gravity anomaly as a guide, rather than an iterative procedure. If necessary, the depth to bedrock can then be adjusted and the procedure repeated.

Plate 6 is the depth to Nogales Formation computed using the residual gravity anomaly grid (pl. 4), the depth to bedrock grid (pl. 5) and the control grid described above. Plate 6 shows that areas where the upper basin fill is thicker than 500 m are rather restricted. The largest area is near Amado, the next largest is near Tubac, and there are two smaller areas north of Nogales. In Part 1 of this report (fig. 2) these areas of thicker basin fill are named the Amado subbasin, Tubac subbasin, Rio Rico subbasin, and Nogales subbasin.

Although there is some variation about the control points, in general the agreement with control values is good. Some areas have several control points within a one-km grid cell and the editing process assigns a value to the grid point equal to the last one in the list falling in that cell. This is not a serious difficulty because from field observations we know that the variations in the degree of cementation of the Nogales Formation and the possibility of relief on the contact of the order of 100 m mean that we can only estimate an average depth in any case. Real variations in the physical properties of the basin units probably preclude any more accurate knowledge of the interface over small areas.

Finally, we evaluated the area east of the Santa Cruz River and south of Sonoita Creek to the International border for possible subbasins. Existing gravity data (pl. 4) do not indicate any significant subbasin in this area. The new aeromagnetic data, however, suggest the presence of a narrow southeast-trending half graben east of Mount Benedict. The graben appears to be 1-2 km wide, and with depths to bedrock computed from the aeromagnetic data of about 300m. The feature is shown in figure 9.

## Summary

Based on reasonable approximations, we have constructed a basin-fill model that satisfies constraints from geologic, well log, gravity and magnetic anomaly data. This model indicates that within the study area, the only areas of significantly thick upper basin fill are in the areas of Amado, Tubac, and Nogales Wash. The Sopori basin may have a small area of significantly thick upper basin fill on its eastern side adjacent to the Tumacacori Mountains.

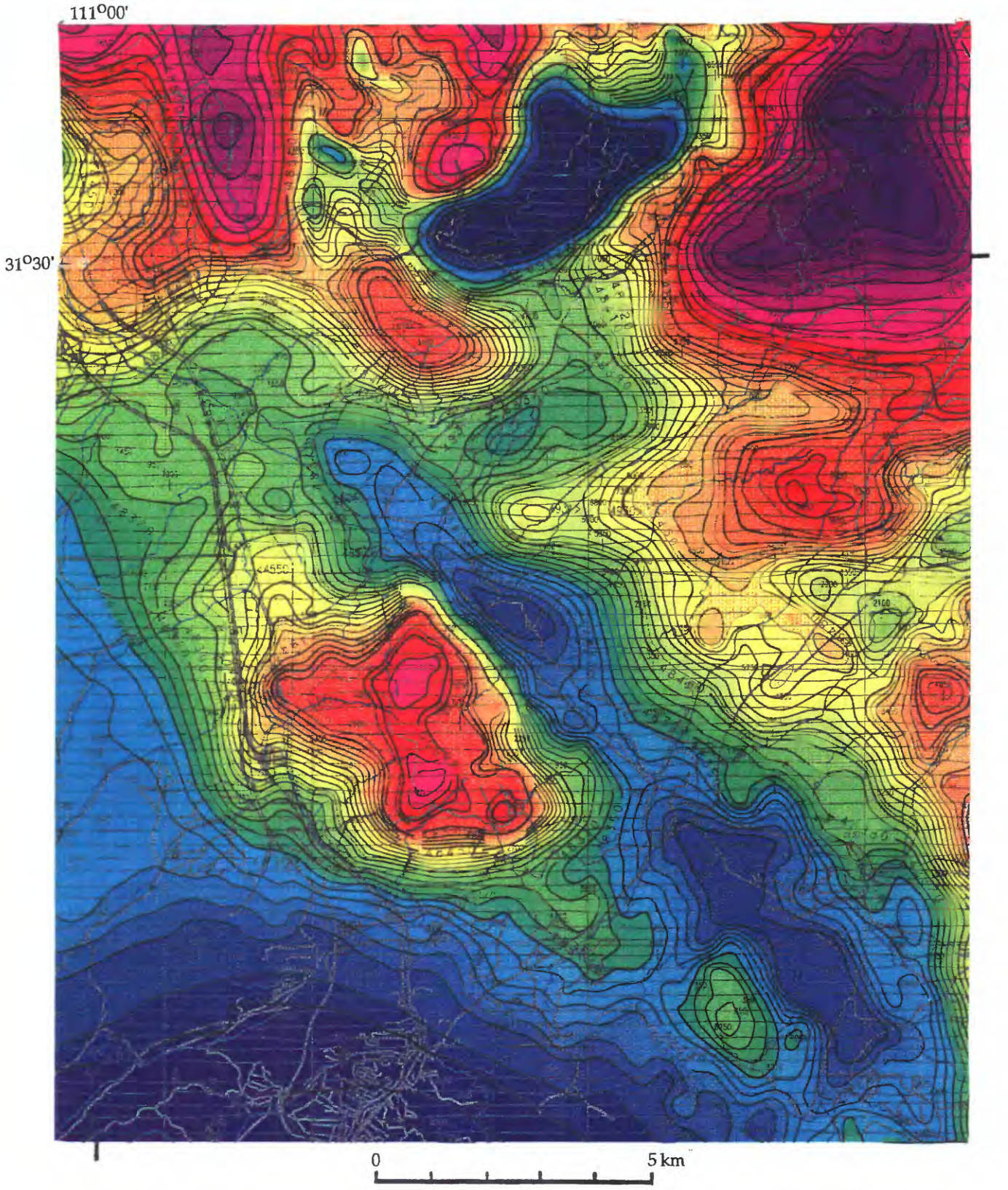


Figure 9. Aeromagnetic map of the Mt. Benedict area showing the narrow half graben to the east along the Mt. Benedict fault. Red colors are relative magnetic highs; blue colors are relative magnetic lows. Compare with figure 1 for location of roads and streams.

## References


Balcer, R.A., 1984, Stratigraphy and depositional history of the Pantano Formation (Oligocene-early Miocene), Pima County, Arizona: Tucson, University of Arizona M.S. thesis, 107 p.

Cooper, J.R., 1973, Geologic map of the Twin Buttes quadrangle, southwest of Tucson, Pima County, Arizona: U.S. Geological Survey Miscellaneous Investigations Series Map I-745, scale 1:48,000.

Dickinson, W.R., 1991, Tectonic setting of faulted Tertiary strata associated with the Catalina core complex in southern Arizona: Geological Society of America Special Paper 264, 106 p.

Drewes, Harald, 1971, Geologic map of the Mount Wrightson quadrangle, southeast of Tucson, Santa Cruz and Pima Counties, Arizona: U.S. Geological Survey Miscellaneous Investigations Series Map I-614, scale 1:48,000.

----------, 1972, Cenozoic rocks of the Santa Rita Mountains, Southeast of Tucson: U.S. Geological Survey Professional Paper 746, 66 p.

----------, 1980, Tectonic map of southeast Arizona: U.S. Geological Survey Miscellaneous Investigations Series Map I-1109, scale 1:125,000.

Duska, L., 1958, Maximum gravity effect of certain solids of revolution: Geophysics, v. 23, p. 506-519.

Gettings, M.E., 1996, Aeromagnetic, radiometric, and gravity data for Coronado National Forest, *in* du Bray, E.A., ed., Mineral resource potential and geology of Coronado National Forest, Southeastern Arizona and Southwestern New Mexico, U.S. Geological Survey Bulletin 2083-D, p. 70-101.

Helmick, W.R., 1986, The Santa Cruz River terraces near Tubac, Santa Cruz County, Arizona: Tucson, Universtiy of Arizona M.S. Thesis, 96 p.

Houser, B.B., Richter, D.H., and Shafiqullah, M., 1985, Geologic map of the Safford quadrangle, Graham County, Arizona: U.S. Geological Survey, Miscellaneous Investigations Series Map I-1617, scale 1:48,000.

Litinsky, V.A., 1989, Concept of effective density -- key to gravity depth determinations for sedimentary basins: Geophysics, v. 54, p. 1474-1482.

Nelson, F.J., 1963, The geology of the Pena Blanca and Walker Canyon areas,Santa Cruz County, Arizona: Tucson, University of Arizona M.S. Thesis, 82 p.

Parasnis, D.S., 1952, A study of rock densities in the English Midlands: Monthly Notices of the Royal Astronomical Society, Geophysical Supplement, v. 6, p. 252-271.

Saltus, R.W., and Jachens, R.C., 1995, Gravity and basin-depth maps of the Basin and Range Province, Western United States: U.S. Geological Survey Geophysical Investigations Map GP--1012, scale 1:2,500,000.

Simons, F.S., 1974, Geologic map and sections of the Nogales and Lochiel quadrangles, Santa Cruz County, Arizona: U.S. Geological Survey Miscellaneous Investigations Series Map I-762, scale 1:48,000, pamphlet 9 p.

Tucci, Patrick., Schmoker, J.W., and Robbins, S.L., 1982, Borehole-gravity surveys in basin-fill deposits of central and southern Arizona: U.S. Geological Survey Open-File Report 82-473, 23 p.

# APPENDIX

## WELL-NUMBERING SYSTEM

The well numbers used by the U.S. Geological Survey in Arizona are in accordance with the Bureau of Land Management's system of land subdivision. The land survey in most of Arizona is based on the Gila and Salt River meridian and base line, which divide the State into four quadrants. These quadrants are designated counterclockwise by the capital letters A, B, C, and D. All land northeast of the point of origin is in A quadrant, that northwest in B quadrant, that southwest in C quadrant, and that southeast in D quadrant. The first digit of a well number indicates the township, the second the range, and the third the section in which the well is situated. The lowercase letters a, b, c, and d after the section number indicate the well location within the section. The first letter denotes a particular 160-acre tract, the second a 40-acre tract, and the third a 10-acre tract. These letters also are assigned in a counterclockwise direction, beginning in the northeast quarter. If the location is known to within the 10-acre tract, three lowercase letters are shown in the well number. In the example shown , well number (D–4–5)19caa designates the well as being in the NE¼NE¼SW¼ sec. 19, T. 4 S., R. 5 E. Where there is more than one well within a 10-acre tract, consecutive numbers beginning with 1 are added as suffixes.

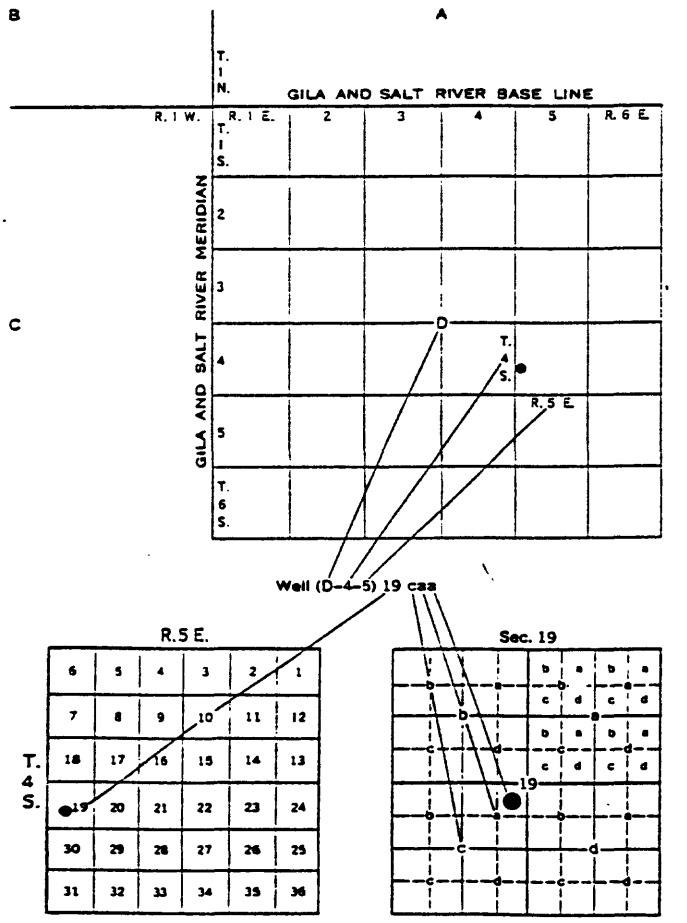


Well-numbering system in Arizona.

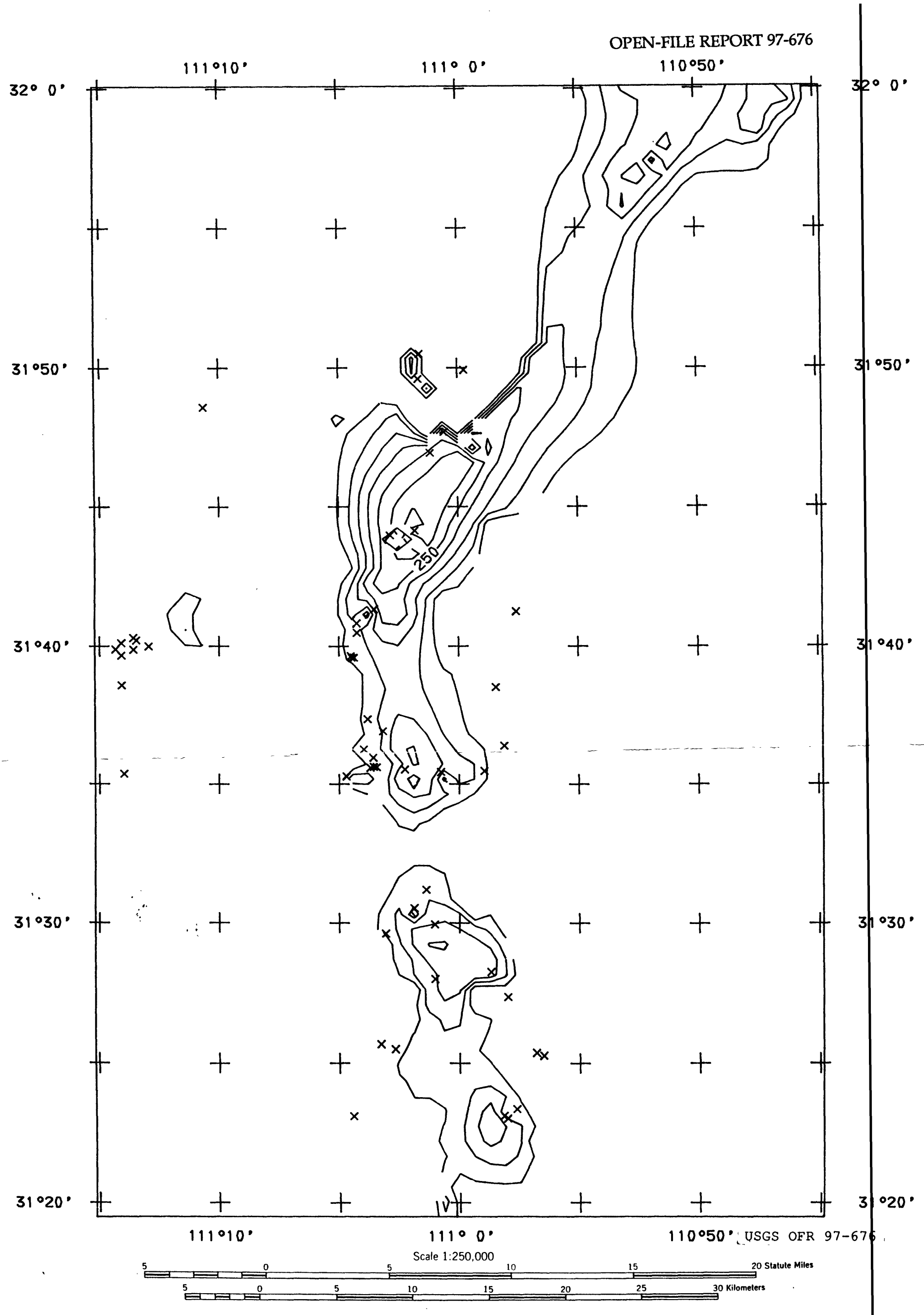


Plate 6. Depth to the interface between the upper basin fill unit and the Nogales Formation for the study area in meters estimated from the residual gravity anomaly field of plate 4 and constrained by drillhole and surface geologic information. Contour interval 50 m; symbols (x) show the location of drillholes used to constrain the solution. Shallowest contour value is 50 m.

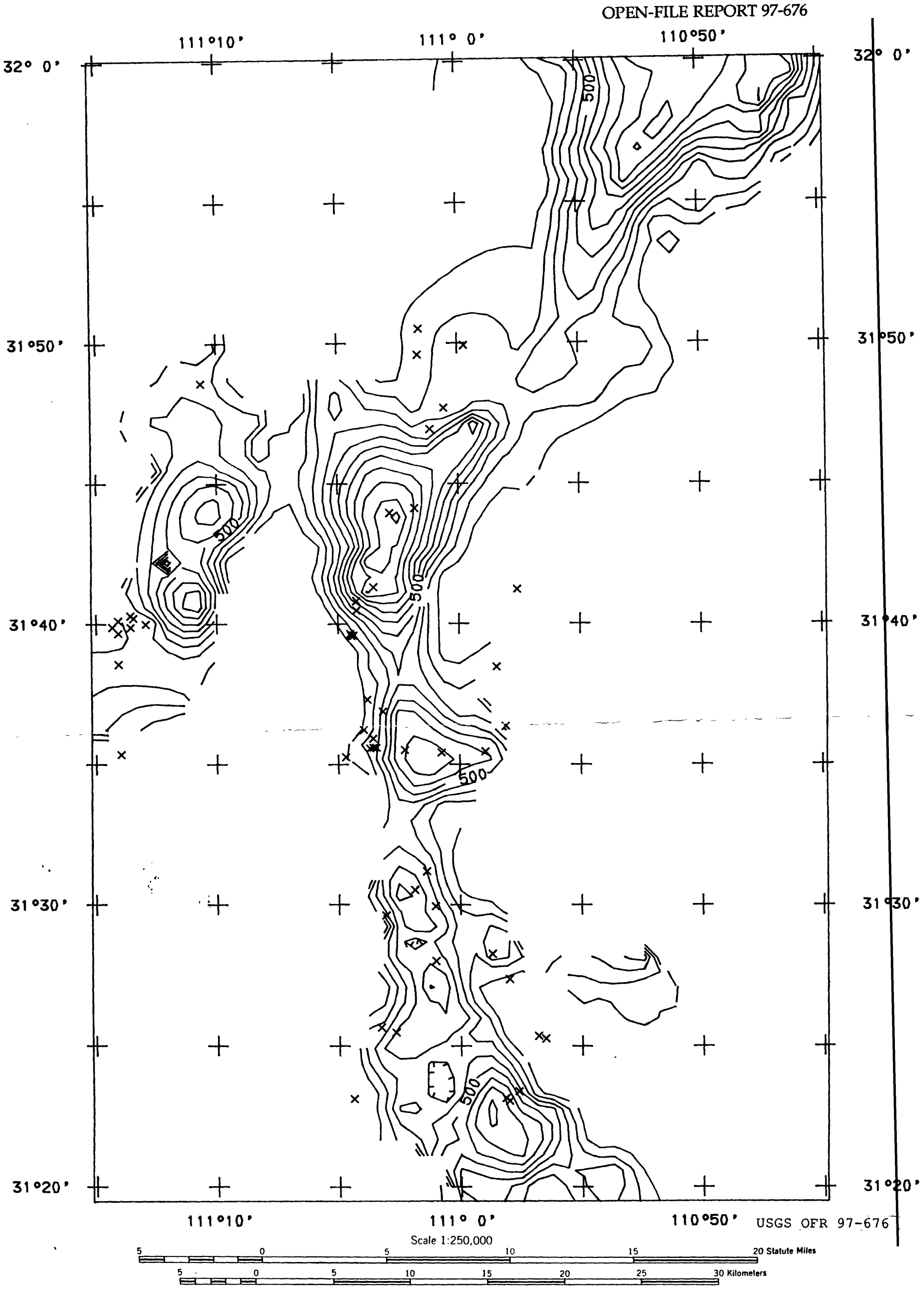


Plate 5. Depth to bedrock in meters for the study area estimated from the residual gravity anomaly field of plate 4 and constrained by drillhole and surface geologic information. Contour interval 100 m; symbols (x) show the location of drillholes used to constrain the solution. Shallowest contour value is 100 m.

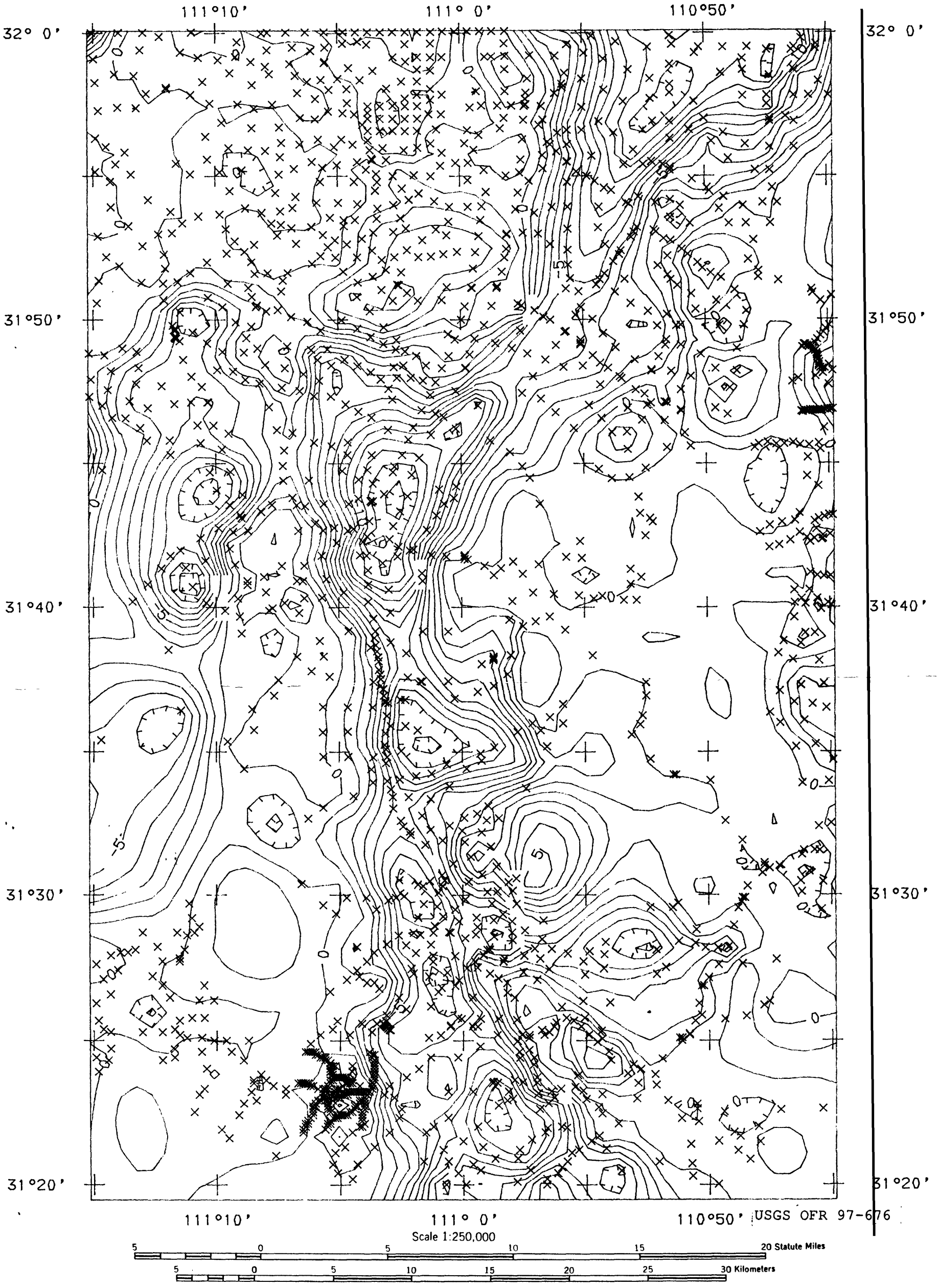


Plate 4. Residual gravity anomaly field for the study area computed by sutracting the regional anomaly field of plate 3 from the complete Bouguer gravity anomaly field of plate 1. Contour interval is 1 mGal; symbols (x) show the location of gravity stations. Hatchured closed contours distinguish relative minima in the anomaly field.

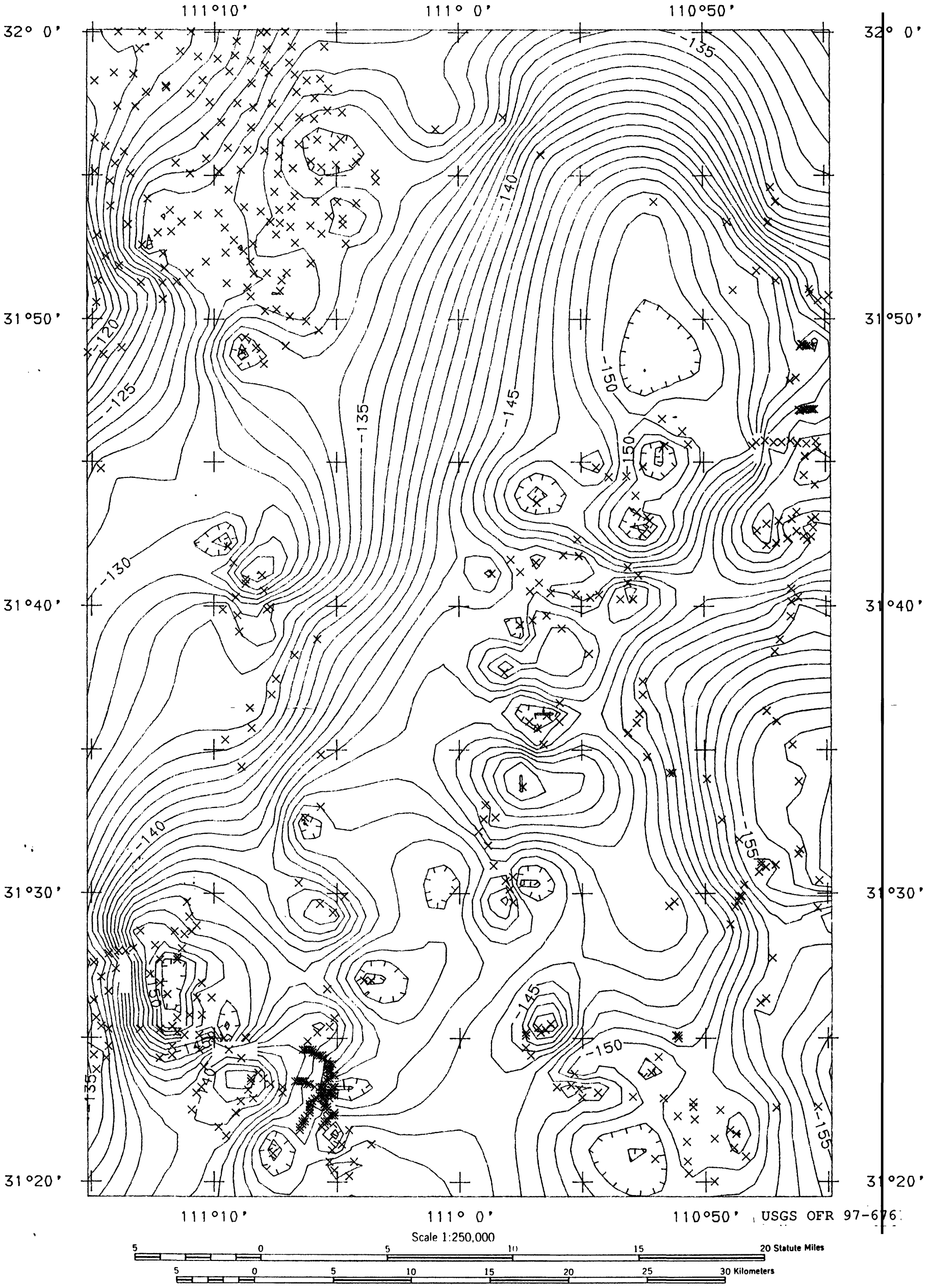


Plate 3. Regional gravity anomaly field for the study area derived from using only stations located on bedrock. Contour interval is 1 mGal; symbols (x) show the location of gravity stations. Hatchured closed contours distinguish relative minima in the anomaly field.

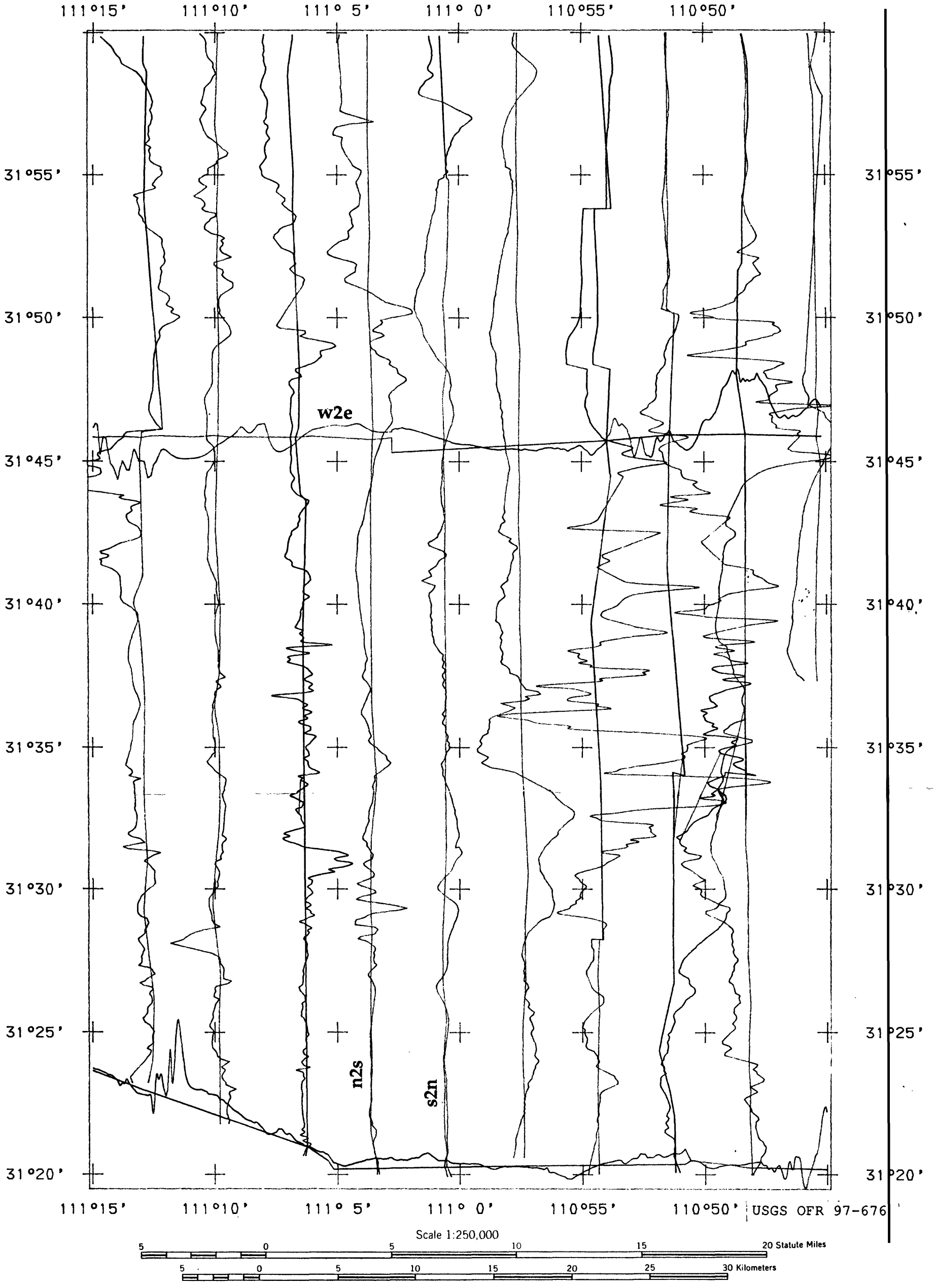


Plate 2. National Uranium Resources Evaluation (NURE) aeromagnetic profiles for the upper Santa Cruz Valley and surrounding areas. Flight paths are shown as piecewise linear line segments, and the aeromagnetic anomaly is plotted approximately perpendicular to the flight path with the flight path as a base value anomaly. For approximately north-south flight paths, a deflection to the east is a positive anomaly, deflection to west is a negative anomaly. For approximately east-west flight paths, a deflection to the north is a positive anomaly, deflection to the south is a negative anomaly. The flight path anomaly value is -250 nanoTesla (nT), and the scale for the aeromagnetic anomaly is 250 nT per minute of latitude. Lines n2s, s2n, and w2e are over part of the basin and were used for depth to magnetic source computations.

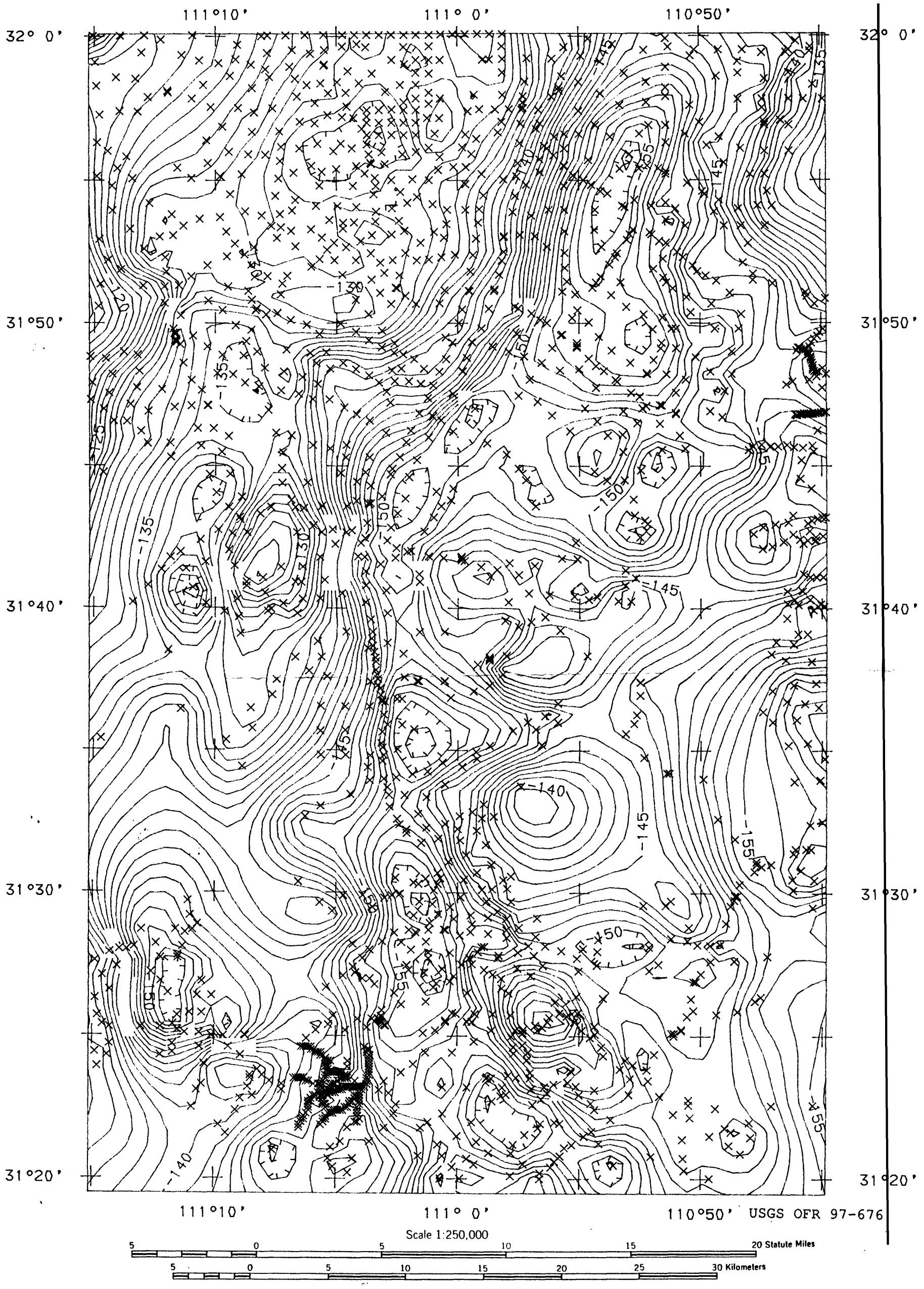


Plate 1. Complete Bouguer gravity anomaly map of the upper Santa Cruz Valley and surrounding areas. Contour interval is 1 mGal; symbols (x) show the location of gravity stations. Hatchured closed contours distinguish relative minima in the anomaly field.